

## Crustal thickening by tectonic wedging of the Ganderian rocks, southern New England, USA: Evidence from cataclastic zircon microstructures and U–Pb ages



Robert P. Wintsch <sup>a,\*</sup>, Keewook Yi <sup>b</sup>, Michael J. Dorais <sup>c</sup>

<sup>a</sup> Department of Geological Sciences, Indiana University, Bloomington, IN 47401, USA

<sup>b</sup> Division of Earth and Environmental Sciences, Korea Basic Science Institute, 162 Yeongudanji-ro, Ochang, Cheongwon, Chungbuk 363-883, Republic of Korea

<sup>c</sup> Department of Geological Sciences, Brigham Young University, Provo, UT 84602, USA

### ARTICLE INFO

#### Article history:

Available online 21 August 2014

#### Keywords:

Tectonic wedging  
Zircon cataclasis  
Alleghanian orogeny  
Appalachian tectonics

### ABSTRACT

Zircon grains in granites from Avalonian and Ganderian rocks in southern New England host brittle internal structures that are interpreted here to show the host rocks to be allochthonous. Significant among these structures are inherited cores that are commonly fractured and even dismembered. This intense fracturing is interpreted as reflecting an important cataclastic event. The maximum age of fracturing is constrained to be younger than the age of the youngest broken magmatic core:  $360 \pm 4$  Ma. The minimum age must be older than the oldest zircon rim that heals these fractures: that is, Early Permian. The occurrence of cataclastic zircon requires that these rocks were relatively cold (i.e. in the upper crust) during the Carboniferous and therefore were not involved in the pervasive high-grade Acadian metamorphism. The present map pattern of inter-tonguing high-grade and low-grade slices of peri-Gondwanan rocks shows that they were assembled by crustal-scale tectonic wedging. The consequent thickening ultimately led to anatexis in the lower slices during the Permian. Thus, evidence for cataclasis of zircon grains from the Avalon and Gander terranes of southern New England suggests that these peri-Gondwanan terranes remained outboard of Laurentia during the well-documented Early Devonian Acadian orogeny and were first fully accreted to North America during the Alleghanian (Permian) orogeny.

© 2014 Elsevier Ltd. All rights reserved.

### 1. Introduction

One characteristic of all orogenic belts is thickened crust. Several mechanisms of crustal thickening have been proposed, including deeply rooted thrust and/or fold nappes (e.g. Hubbard and Shaw, 2009), low viscosity crustal channel flow (e.g. Beaumont et al., 2004), and tectonic wedging (e.g. Moore and Wiltschko, 2004). As more orogens are investigated using deep seismic profiles, models of mantle delamination and crustal single and(or) double wedging have been proposed (e.g. van der Velden et al., 2004). All studies of modern and active mountain belts are limited by the lack of physical evidence of proposed lower crustal processes; these studies rely in part on numerical models and on remote sensing. In

this study, we have examined rocks that were buried to mid-crustal levels in an over-thickened crust during the Permian Alleghanian orogeny. Rocks buried to >40 km are now exposed at the surface (Wintsch et al., 2003) and can be examined to investigate the processes that may have operated during their loading. Although the rocks are well exposed at the surface (Rodgers, 1985), the recrystallization accompanying the very high grades of metamorphism and anatexis have modified and even destroyed the structures developed at the time of loading. Unique among minerals, zircon is capable of preserving structures as well as isotopic compositions in spite of such high-grade metamorphism. Studying both isotopic and microstructural characteristics of zircons in southern New England has enabled us to identify the processes of intra-crustal wedging.

We discovered this wedging while testing the hypothesis that Early Devonian metamorphism associated with the Acadian orogeny (Fig. 1) was caused by the accretion of the Avalon terrane to the margin of composite Laurentia (e.g. Bradley, 1983). This event is

\* Corresponding author. Department of Geological Sciences, Indiana University, 1001 E 10th St., Bloomington, IN 47405, USA. Tel.: +1 8128554018, +1 8128555582.

E-mail address: [wintsch@indiana.edu](mailto:wintsch@indiana.edu) (R.P. Wintsch).

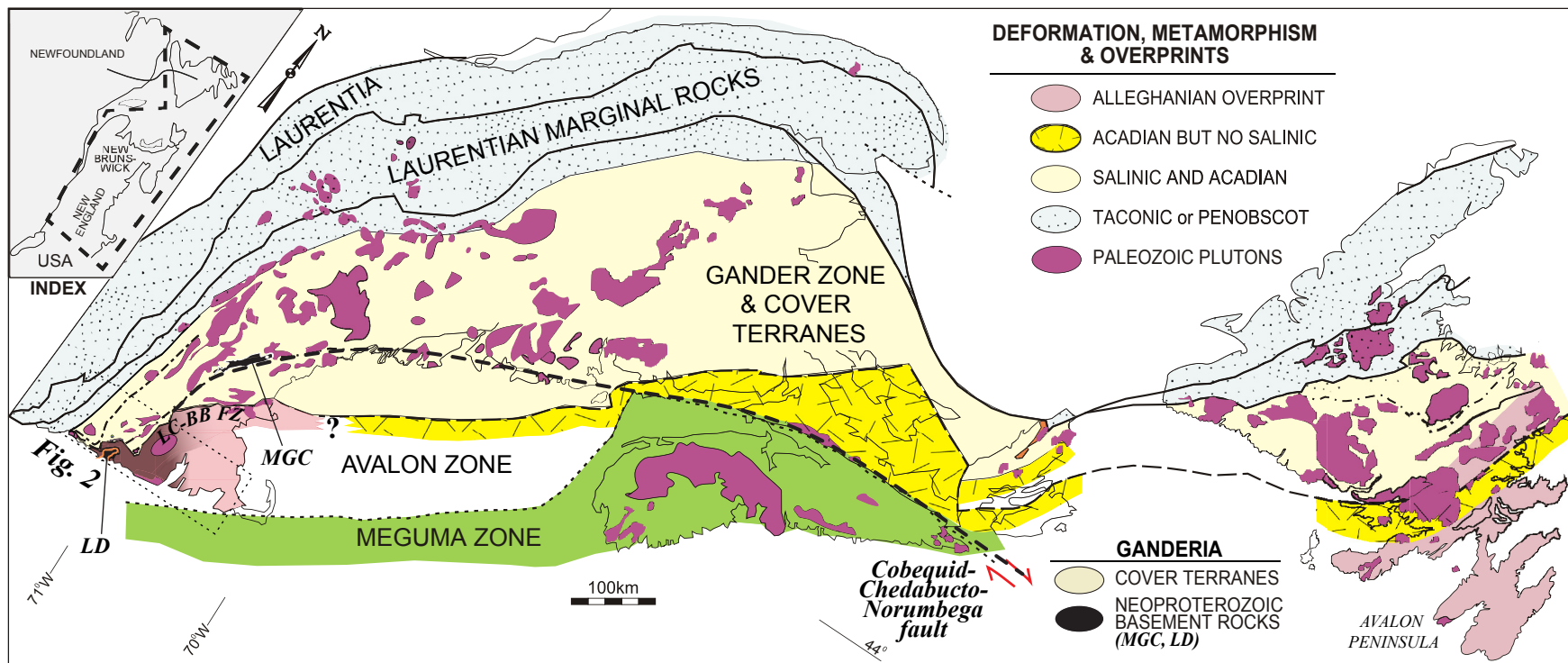


**Fig. 1.** A generalized map of the northern Appalachians showing the distribution of metamorphic effects on major terranes, and the locations of plutonic rocks (modified from van Staal, 2005). Peri-Gondwanan terranes include the Gander (pale yellow), Avalon, and Meguma zones. Peri-Laurentian marginal terranes are colored pale blue. Ages of deformation and metamorphic overprint are indicated with stipple (Taconic or Penobscot), Acadian without Salinic (confetti) and Alleghanian (shades of pink increasing with metamorphic grade). The dotted box shows the location of Fig. 2. Abbreviations are: LC-BB FZ, Lake Char-Bloody Bluff fault zone; LD, Lyme dome; MGC, Massabesic Gneiss complex. The latter two (black) bodies are Neoproterozoic and interpreted to be Gander basement (see text). (For interpretation of the references to color in this figure legend, the reader is referred to the web version of this article.)

best documented along the St. Lawrence promontory of Newfoundland where the collision shortened associated volcanic arc units and inverted backarc basins (e.g. van Staal et al., 2009). Structures throughout the crust of Newfoundland revealed by deep seismic profiling (van der Velden et al., 2004) suggest that the crust there was thickened by double wedging of crustal blocks representing Laurentia, Ganderia, and Avalonia.

In contrast, direct evidence for the docking of Avalon as the cause of the Acadian orogeny in southern New England is surprisingly lacking in spite of arguments to the contrary (Robinson et al., 1998). Neoproterozoic Avalonian rocks in eastern Massachusetts (and Newfoundland's Avalon Peninsula, Fig. 1) are essentially unmetamorphosed, but to the southwest both Avalonian rocks and overlying Pennsylvanian terrestrial foreland sediments show a prograde metamorphism that reached staurolite-kyanite grade at ~285 Ma (e.g. Dallmeyer, 1982; Hermes et al., 1994). In coastal Rhode Island and Connecticut, a regional migmatite terrane prevails in peri-Gondwanan rocks (e.g. Lundgren, 1966; Fig. 2). Thus, it is possible that geochronological evidence for an Acadian metamorphism was destroyed by subsequent Permian high-grade metamorphism. Alternatively, it is possible that these rocks were not fully amalgamated to marginal Laurentia until the Permian during the Alleghanian orogeny (e.g. Dorais et al., 2012). This hypothesis requires that the Avalonian rocks now exposed in southeastern New England were outboard of any Acadian collision and remained there, undeformed, until the late Paleozoic. It leaves open the question of whether a more proximal portion of Avalonia was accreted to Laurentia in pre-Carboniferous times.

The present study was undertaken to determine the ages of inherited cores, igneous mantles, and metamorphic rims in zircons from Alleghanian granitic rocks in southeastern New England. Four granitic rocks were collected along an east-to-west transect with the goal of dating zircon and its inheritance concerning the tectono-magmatic evolution of Ganderia and Avalonia. Zircons

were the target mineral because inherited cores and metamorphic overgrowths have been found both locally (Aleinkoff et al., 2007; Walsh et al., 2007) and regionally (Zartman, and Hermes, 1987; Walsh et al., 2004; Wintsch et al., 2007). Moreover, Devonian metamorphic zircon in amphibolite has survived anatexitic metamorphic conditions in the Massabesic Gneiss complex, southern New Hampshire (Dorais et al., 2012; MGC, Fig. 1), in an apparent pop-up structure associated with an extension of the Cobequid-Chedabucto-Norumbega fault zone (Fig. 1). We initiated this study specifically to search for evidence of the Early Devonian (Acadian) accretion of Avalonia to southeastern New England. Samples were selected at the eastern, central, and western limits of what has been interpreted as Neoproterozoic peri-Gondwanan (Avalonian) terranes (e.g. Rodgers, 1985). Our results do not support an Early Devonian metamorphic recrystallization event in these rocks. However, the microstructures within zircon grains, in combination with the isotopic data, do support crustal wedging as a major cause of late Paleozoic orogenesis in southeastern New England.

## 2. Geologic and tectonic setting

Southeastern New England has been divided into several lithostratigraphic-tectonic terranes based on differences in lithology, metamorphic grade, and cooling history (e.g. Wintsch et al., 1992, 1993; Hibbard et al., 2006). These include the major divisions of Laurentia and marginal Laurentian rocks on the west and Gander with its cover, and Avalon and Meguma to the east (Fig. 1). Within the Gander zone are the cover terranes Bronson Hill, Central Maine, Merrimack, and Putnam-Nashoba (Fig. 2), each bounded by ductile faults. Most of these terranes form slices that are dipping, and apparently tapering, to the west. The Lake Char-Bloody Bluff fault zone (LC-BB FZ, Fig. 1) separates the easternmost Avalon terrane from the overlying Putnam-Nashoba terrane, but the trace

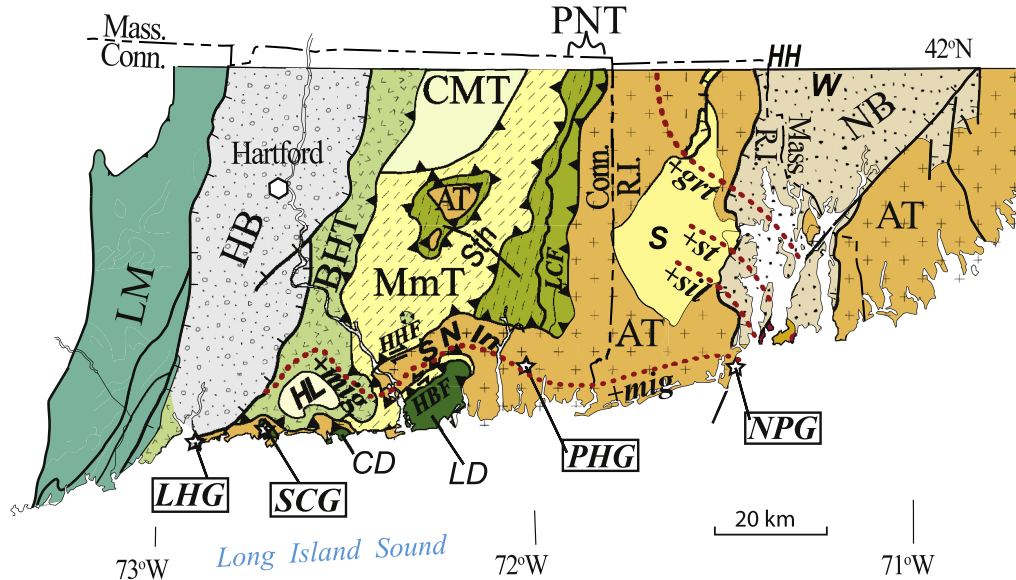


**Fig. 2.** A generalized geological map of southern New England, showing terranes between the Laurentian margin (LM) on the west and the Avalon terrane (AT, + pattern) on the east (modified from Hibbard et al., 2006). Ordovician and Silurian Gander cover terranes east of the Hartford basin (HB) are the Bronson Hill terrane (BHT, v pattern), Central Maine terrane (CMT), Merrimack terrane (MmT, NE dashes), and Putnam-Nashoba terrane (PNT) dominated by the Silurian Tatnic Hill Formation (Sth, NNE dashes). The Pennsylvanian Narragansett basin (NB) is also identified. The garnet (grt), staurolite (st), sillimanite (sil) isograds and the northern limit of abundant migmatite (mig) are indicated with red dotted lines. Rocks of the Lyme dome (LD) and Clinton dome (CD) are late Proterozoic Gander basement rocks. The Devonian Scituate (S) and Mississippian Hidden Lake (HL) plutons are indicated. The location of the Wamsutta Formation is labeled 'W.' The locations of analyzed samples of Light House Gneiss (LHG), Stony Creek Granite (SCG), Potter Hill Gneiss (PHG), and the Narragansett Pier Granite (NPG) are indicated by the stars. The Avalonian Selden Neck indenter (SNIn) wedged between Gander metasedimentary cover and Gander Lyme dome basement rocks along the upper Honey Hill (HHF) and Lake Char (LCF) faults and the lower Hunts Brook fault (HBF). For other discussion see text. (For interpretation of the references to color in this figure legend, the reader is referred to the web version of this article.)

of this fault turns from southward to westward, and the name changes to the Honey Hill fault (HHF, Fig. 2). Some units in the Avalon footwall also follow this south then west outcrop pattern. In fact, the general NNE strike of the terranes east of the Hartford basin (HB, Fig. 2) is interrupted by the generally east-trending Honey Hill fault. This fault, and most of the units and structures south of it, dip and plunge northward.

The cover terranes that were deposited upon Neoproterozoic magmatic and volcanic rocks of Gander ‘basement’ are now understood to be allochthonous. This interpretation is based on lithostratigraphic and time-stratigraphic correlations to the north where the cover rocks are mapped as autochthonous on Gander ‘basement’ (e.g. Hibbard et al., 2006; Dorais et al., 2012; van Staal and Barr, 2012). The fact that in eastern Connecticut these high-grade Gander cover terranes metamorphosed during the Acadian orogeny now lie on Avalonian rocks rather than on Ganderian basement requires a major thrust of all the cover rocks over Avalonia, and over each other (Wintsch et al., 1993; Walsh et al., 2007). If this thrusting event occurred during the Early Devonian Acadian orogeny, then the peri-Gondwanan rocks of southern coastal New England, including Avalonian rocks, should record the Early Devonian anatetic conditions of the cover rocks. Such high-grade conditions have been demonstrated in the Early Devonian ages of zircon and monazite of the Tatnic Hill and Merrimack slices (Wintsch et al., 2007) and the Central Maine slice (Eusden and Barreiro, 1988; Thomson et al., 1992; Wintsch et al., 2009). If thrusting of Gondwanan cover terranes over Avalon did not occur until the Alleghanian as proposed by Wintsch and Sutter (1986), then only Neoproterozoic and late Paleozoic ages should be preserved in zircon from Avalonian rocks.

The peri-Gondwanan rocks analyzed here form a discontinuous band of high-grade rocks from southern Rhode Island to the Hartford basin where regional anatetic conditions prevail (e.g. Lundgren, 1966; Aleinikoff et al., 2007; mig., Fig. 2). The rocks are highly deformed and exhibit several generations of fabric development and folding, each associated with partial melting. Zircon ages show that these stages all occurred in the Permian (Walsh et al., 2007), and thus the deformation and anatexis are related to the Alleghanian orogeny. This study further tests this interpretation by analyzing the petrography and geochronology of zircon in four granitoids from the southern coast of New England.

### 3. Methods

Zircon was extracted from the rocks by crushing and sieving, followed by density separation in methylene iodide, and magnetic separation. Standard and unknown zircon grains ranging from 63 µm to 245 µm in length were mounted in epoxy resin, ground to expose the interiors of the grains, and polished. Grains were studied by transmitted and reflected light petrography, and by cathodoluminescent (CL) and backscattered electron (BSE) imaging obtained using a JEOL 6610LV scanning electron microscope. Many grains contain complicated internal structures. We use the term ‘overgrowth’ to refer to any zircon mantling an interior zone, and the term ‘rim’ to refer to the outer-most margin of a grain. Qualitative chemical analysis of zircon and its inclusions was performed using an INCA X-ray energy dispersive spectrometer (EDS). Minerals were identified by comparison with natural mineral standards. Zoning in zircon with relatively low U contents (<1000 ppm) was most conspicuous in CL imaging, whereas internal structures in grains with higher U concentrations were better revealed by BSE imaging. Exploratory electron microprobe analysis of the oscillatory zones was performed using a JEOL JXA-8100. Operating conditions were: current = 50 nA, accelerating potential = 15 kV, beam width = 1 µs, dwell times = 500 ms. Linear variations of Zr, Si, Fe, Ti,

Hf, Y, and F were measured with a 0.1 µm interval and 0.5 s in each step. The measured  $^{206}\text{Pb}/^{238}\text{U}$  ratio was calibrated using standard FC-1 zircons (1099.0 Ma; Paces and Miller, 1993). Zircon standard SL13 (U = 238 ppm) was used only for calibration of U and Th concentrations.

Zircon U–Pb dating was carried out using the SHRIMP-IIe/MC at the Korean Basic Science Institute. The analytical procedures for SHRIMP dating were mostly laid out in Williams (1998). A 20–25 µm spot size was used for all analyses under a negative ion oxygen beam ( $\text{O}_2^-$ ) with a 3–4 nA beam current. The data were collected in sets of five iterative scans through the mass stations for each isotope. Common Pb ( $^{206}\text{Pb}_{\text{C}}$ ) for the  $^{206}\text{Pb}^*/^{238}\text{U}$  ages was corrected on the basis of the measured  $^{207}\text{Pb}/^{206}\text{Pb}$  ratio (Williams, 1998). FC-1 standard grains (1099.0 Ma; Paces and Miller, 1993) were repeatedly analyzed after three analyses of unknown grains, and the measured  $^{206}\text{Pb}/^{238}\text{U}$  ratio was calibrated using this standard. Zircon standard SL13 (U = 238 ppm) was used only for calibration of U and Th concentrations.

Data reduction and processing were carried out using the Squid 2.50 and Isoplot 3.71 programs of Ludwig (2008, 2009). The routine for drift correction for secular variation in Pb/U ratios of repeated FC-1 standard analyses was applied. The age ( $\pm 2\sigma$ ) of each specimen was calculated by determining the weighted average of concordant  $^{207}\text{Pb}$ -corrected  $^{206}\text{Pb}^*/^{238}\text{U}$ . Tera-Wasserburg concordia plots used uncorrected ratios of  $^{206}\text{Pb}/^{238}\text{U}$  and  $^{206}\text{Pb}/^{207}\text{Pb}$ . All uncertainties in the tables and diagrams below are given in  $1\sigma$ . It should be noted that some analysts would have avoided analyzing the zircons studied here because their complicated, fine-scale structures render them not well-suited for precise dating.

### 4. Results

The four granites studied have been mapped as simple Alleghanian intrusive rocks (e.g. Rodgers, 1985). However, most of the zircon grains within these granites contain complex internal structures that demonstrate a complicated crystallization history. SHRIMP analysis of these zircons followed only cursory BSE and CL inspection of the grains at low magnification to avoid damage to the epoxy mounting medium. A much more thorough SEM examination was made subsequent to SHRIMP analysis. Some analyses were subsequently rejected because the analytical spot overlapped more than one compositional domain or sampled a crack. Table 1 includes all the reliable analyses but does not include compromised analyses. However, some of the analyses show high common lead concentrations, and yield imprecise ages. In spite of this the analytical data in the context of the cataclastic structures of the zircon grains do allow us to draw conclusions about the late Paleozoic tectonic history of these rocks.

The four samples contain many grains with multiple stages of growth, dissolution, and overgrowth, and with contrasting concentrations of U and Pb. Zircons from the Narragansett Pier Granite show many of these features, and so are described first and in detail. Descriptions of other samples refer to these zircons as appropriate.

#### 4.1. Narragansett Pier Granite

The Narragansett Pier Granite is a tan-to-yellow weathering, very weakly foliated, coarse-grained granite with minor granodiorite and quartz monzonite (Hermes et al., 1994). The granite is well exposed along the southwest shore of Narragansett Bay (Martin, 1925; Nichols, 1956; Hozik, 1988; Hermes et al., 1981; Reck and Mosher, 1988; Fig. 2). Our sample was collected far from local pegmatites and xenoliths exposed there.

**Table 1**

SHRIMP U–Th–Pb data for zircon from coastal southern New England.

Sample <sup>a</sup> (location)	Measured $^{204}\text{Pb}/^{206}\text{Pb}$	Measured $^{207}\text{Pb}/^{206}\text{Pb}$	% Common $^{206}\text{Pb}$	U (ppm)	Th/U	$^{206}\text{Pb}^{\text{b}}/^{238}\text{U}$ (Ma)	Err <sup>c</sup> (Ma)	$^{238}\text{U}^{\text{d}}/^{206}\text{Pb}$	Err <sup>c</sup> (%)	$^{207}\text{Pb}^{\text{d}}/^{206}\text{Pb}$	Err <sup>c</sup> (%)	Notes <sup>e</sup>
<i>Narragansett Pier Granite, Hazard Street, Narragansett Pier, R.I. [41°24'53.42"N, 71°27'11.04"W]</i>												
NP-1.1	5.1E-4	0.0515	—	76	1.33	292	4	21.8	2.38	0.0440	34.4	C2 oz
NP-2.1	3.3E-4	0.0522	0.03	443	0.71	285	2	22.3	0.75	0.0473	5.0	C1 oz
NP-5.1	1.6E-4	0.0546	0.35	266	0.33	280	2	22.6	0.91	0.0522	6.7	C1 sz
NP-5.2	1.4E-4	0.0521	0.01	569	0.51	287	2	22.0	0.72	0.0501	3.8	C2 sz
NP-6.1	8.5E-4	0.0612	0.21	63	0.60	585	8	10.7	1.73	0.0487	16.9	C0 br
NP-7.1	7.9E-3	0.1708	14.82	2325	0.31	281	2	22.4	0.66	0.0556	6.5	R2 oz
NP-8.2	3.2E-3	0.1016	6.22	1471	0.12	273	2	23.1	0.97	0.0541	4.9	R1
NP-9.1	1.5E-3	0.0499	—	157	1.70	287	3	22.7	1.46	0.0278	30.9	C1 oz
NP-10.1	6.9E-4	0.0512	—	185	1.06	277	3	23.1	1.24	0.0409	14.1	C2,oz, sc
NP-12.1	7.9E-4	0.0539	0.25	95	2.89	278	3	23.0	1.95	0.0421	29.9	C1 oz
NP-13.1	5.4E-5	0.0504	—	331	0.44	289	2	21.8	0.86	0.0496	6.1	C1 oz sz
NP-14.1	1.1E-3	0.0495	—	74	1.66	283	4	22.8	2.05	0.0335	41.7	C2 oz
NP-16.1	1.6E-4	0.0521	—	187	1.60	291	3	21.7	1.24	0.0498	13.3	C1 oz, sz
NP-18.1	-5.6E-5	0.0496	—	51	1.01	283	5	22.3	2.90	0.0504	38.3	C2
NP-19.1	-3.1E-5	0.0506	—	95	1.23	276	4	22.8	1.85	0.0511	21.6	C2 oz sz
NP-21.1	-1.5E-5	0.0504	—	187	1.51	285	6	22.2	2.29	0.0507	12.4	C2 oz
NP-22.1	-5.4E-5	0.0602	0.02	1063	0.67	604	4	10.2	0.67	0.0610	1.1	C0 + C1 oz
NP-22.2	5.1E-5	0.0605	—	921	0.52	623	4	9.9	0.67	0.0597	1.3	C0 + C2 oz
NP-23.2	-6.2E-4	0.0522	0.02	159	0.99	287	3	21.7	1.22	0.0612	9.0	C2 oz
NP-26.1	3.9E-4	0.0557	—	143	0.78	484	5	12.9	1.19	0.0500	9.3	C0 + C1 oz
NP-27.1	-4.5E-4	0.0519	—	189	1.50	283	3	22.1	1.16	0.0584	9.0	C1 oz
NP-28.1	-8.5E-4	0.0527	0.07	183	1.57	290	3	21.4	1.15	0.0649	7.6	C2 oz
NP-29.1	-4.7E-4	0.0531	0.15	248	0.91	282	3	22.1	0.99	0.0599	6.3	C1 oz
NP-30.1	2.3E-4	0.0542	0.26	1516	0.03	288	2	22.0	0.63	0.0509	2.0	R1 oz
NP-31.1	-9.3E-5	0.0529	0.14	290	1.76	276	2	22.8	0.97	0.0543	7.0	C2 oz
NP-32.1	-5.0E-6	0.0603	0.32	307	0.10	515	6	12.0	1.25	0.0603	3.3	C0 + C1 oz
NP-33.1	-5.0E-4	0.0523	0.05	200	1.53	284	3	22.0	1.11	0.0596	7.9	C1 > C2 oz, sz
NP-35.1	2.6E-5	0.0539	0.25	206	1.37	279	3	22.5	1.2	0.0535	6.0	C1 oz
NP-36.1	-6.6E-5	0.0536	0.24	285	1.26	274	3	23.0	1.1	0.0546	5.0	C2 oz
NP-37.1	9.8E-5	0.0535	0.22	166	1.11	276	3	22.8	1.3	0.0521	8.2	C2 oz
NP-38.1	4.0E-5	0.0488	—	133	1.38	286	4	22.1	1.4	0.0482	11.1	C2 oz
NP-39.1	-3.2E-5	0.0526	0.07	193	1.45	284	3	22.1	1.2	0.0530	5.8	C1 oz
NP-40.1	-2.0E-4	0.0545	0.32	138	1.16	280	4	22.4	1.4	0.0573	8.0	C1 oz, sz
NP-40.2	2.6E-3	0.0927	5.11	878	0.11	272	3	23.1	1.0	0.0551	5.9	R1 oz, sz
NP-44.1	2.2E-5	0.0527	0.09	234	1.56	284	3	22.2	1.2	0.0524	5.1	C2 oz
NP-45.1	-9.3E-5	0.0473	—	201	1.61	286	5	22.1	1.9	0.0487	10.4	C1 oz, sz
NP-46.1	-9.0E-5	0.0559	0.51	215	1.52	278	3	22.6	1.3	0.0572	7.6	C1 oz
NP-47.1	1.1E-4	0.0508	—	240	1.17	288	3	22.0	1.2	0.0492	5.0	C1 oz, sz
NP-48.1.ra	9.7E-5	0.0612	0.11	844	0.55	616	8	10.0	1.3	0.0598	1.7	C0 oz
NP-48.2	-7.2E-6	0.0592	—	663	0.48	623	8	9.9	1.3	0.0594	1.6	C0 oz
NP-49.1	-9.2E-5	0.0505	—	499	2.22	281	4	22.4	1.3	0.0519	4.4	C1 oz
NP-50.1	-4.6E-5	0.0512	—	215	1.72	276	4	22.9	1.5	0.0519	7.6	C1 oz
NP-51.1	-1.9E-4	0.0546	0.34	645	0.23	278	3	22.5	1.3	0.0572	3.2	C2 oz
NP-52.1	1.1E-4	0.0510	—	576	0.78	286	4	22.2	1.3	0.0494	4.4	C1 oz
NP-53.1	-4.7E-4	0.0558	0.52	98	1.29	269	5	23.1	2.1	0.0627	14.4	C2 oz
NP-54.1	1.3E-4	0.0517	—	338	0.28	282	4	22.4	1.4	0.0498	5.5	C2 oz
NP-55.1	-5.7E-4	0.0534	0.18	189	1.24	285	4	21.9	1.6	0.0617	7.1	C1 oz
NP-56.1	-9.0E-5	0.0621	0.23	404	0.55	610	8	10.0	1.3	0.0634	2.3	C0 oz
<i>Potter Hill Gneiss road cut at N-bound exit of I95 with Rt. 2, North Stonington, Conn. [41°24'36.48"N, 71°51'18.87"W]</i>												
PH-1.1	6.3E-5	0.0620	0.31	325	0.32	586	5	10.5	0.86	0.0611	2.9	C2 > C1
PH-2.1	1.1E-4	0.0609	0.15	289	0.91	590	5	10.4	0.89	0.0593	3.5	C1 > C2
PH-2.2	-5.2E-4	0.0607	0.55	141	0.31	460	5	13.3	1.26	0.0682	7.3	C2 > C1
PH-3.1	1.1E-3	0.0714	1.60	89	0.51	543	7	11.4	1.56	0.0548	12.9	C1
PH-4.1	1.6E-4	0.0605	0.16	129	0.75	577	7	10.7	1.25	0.0582	7.9	C1
PH-5.1	-1.7E-4	0.0623	0.23	104	0.62	616	8	9.9	1.38	0.0647	7.5	C1
PH-6.1	-4.4E-4	0.0612	0.12	125	0.44	611	7	10.0	1.25	0.0675	6.0	C2
PH-7.1	3.8E-4	0.0640	0.48	99	0.54	604	7	10.2	1.40	0.0584	9.4	C2
PH-8.1	4.8E-5	0.0619	0.19	199	0.43	615	6	10.0	1.05	0.0612	4.8	C2
PH-9.1	3.7E-3	0.1076	6.92	2226	0.04	288	2	21.9	0.66	0.0528	4.2	R
PH-10.1	-1.8E-4	0.0598	0.00	166	0.54	596	6	10.3	1.11	0.0624	5.2	C1 > C2
PH-10.2	1.8E-3	0.0895	4.01	1075	0.36	491	3	12.5	0.68	0.0632	2.7	R1 > C2
PH-11.1	1.9E-3	0.0886	4.13	1106	0.32	420	3	14.7	0.69	0.0610	3.1	R1 > R2
PH-12.1	4.1E-6	0.0606	0.07	1011	0.48	603	4	10.2	0.66	0.0605	1.2	C2
PH-13.2	3.8E-5	0.0605	0.10	1119	0.32	592	4	10.4	0.65	0.0599	1.1	C2
PH-14.1	4.0E-3	0.1186	8.17	1590	0.37	324	6	19.2	2.01	0.0603	5.6	R > C2
PH-14.3	4.1E-3	0.1085	7.12	2108	0.02	261	2	24.3	0.67	0.0482	5.3	R2
PH-15.1	4.2E-3	0.1159	7.51	1687	0.27	416	4	15.0	0.93	0.0553	4.8	C2 + R1
PH-15.2	4.1E-3	0.1194	8.16	1765	0.30	358	3	17.4	0.92	0.0595	3.8	C2 + R2
PH-15.3	2.0E-3	0.0837	3.96	1796	0.03	282	2	22.3	0.65	0.0545	3.4	R
PH-16.1	1.8E-4	0.0628	0.57	581	0.52	534	4	11.6	0.74	0.0602	2.2	C1
PH-16.2	2.6E-3	0.0984	5.22	769	0.41	455	3	13.6	0.74	0.0608	4.1	C2 + R1

**Table 1** (continued)

Sample <sup>a</sup> (location)	Measured $^{204}\text{Pb}/^{206}\text{Pb}$	Measured $^{207}\text{Pb}/^{206}\text{Pb}$	% Common $^{206}\text{Pb}$	U (ppm)	Th/U	$^{206}\text{Pb}^{\text{b}}/^{238}\text{U}$ (Ma)	Err <sup>c</sup> (Ma)	$^{238}\text{U}^{\text{d}}/^{206}\text{Pb}$	Err <sup>c</sup> (%)	$^{207}\text{Pb}^{\text{d}}/^{206}\text{Pb}$	Err <sup>c</sup> (%)	Notes <sup>e</sup>
PH-16.3	2.2E-3	0.0864	4.27	1393	0.01	288	2	21.8	0.67	0.0546	4.7	R1
PH-17.1	1.8E-5	0.0695	0.62	364	0.72	754	8	8.0	1.14	0.0692	1.7	C1
PH-17.2	-1.6E-4	0.0613	0.14	327	0.39	608	5	10.1	0.84	0.0636	2.4	C2
PH-18.1	-2.6E-5	0.0604	0.20	718	0.62	558	4	11.0	0.69	0.0607	1.5	C1 + R
PH-19.2	8.4E-4	0.0728	1.86	598	0.44	516	4	12.0	0.75	0.0606	3.0	C2 R1
PH-21.1	3.0E-5	0.0618	0.21	138	0.75	607	7	10.1	1.20	0.0614	6.7	C2
PH-21.2	-5.9E-6	0.0598	0.04	408	0.54	584	9	10.5	1.60	0.0598	3.9	C1
PH-22.2	4.0E-4	0.0646	1.33	635	0.09	365	3	17.1	0.75	0.0588	3.2	R1 > C2
<b>Stony Creek Granite, Branford, Conn. [41°17'16.36"N, 72°44'37.87"W]</b>												
SC-1.1	6.6E-05	0.0519	—	483	0.21	289	±2	21.8	0.72	0.0510	3.6	R1
SC-1.2	1.7E-04	0.0554	0.25	72	0.55	348	±9	18.0	2.92	0.0529	22.4	C2 > R1
SC-1.3	2.5E-04	0.0563	0.31	76	0.53	363	±4	17.3	1.60	0.0526	16.1	C1
SC-2.1	9.3E-04	0.0459	—	109	0.51	362	±6	17.8	1.46	0.0320	38.9	C1
SC-3.1	2.9E-05	0.0525	0.05	1329	0.32	290	±2	21.8	0.61	0.0521	1.6	R1
SC-4.1	-6.2E-06	0.0526	0.07	718	0.29	289	±2	21.8	0.88	0.0527	2.7	R1
SC-5.1	2.3E-03	0.0897	—	416	0.63	1447	±115	4.1	8.68	0.0564	43.0	Co d oz
SC-5.1 ... dup1	—	0.0519	—	1245	0.43	290	±2	21.7	0.62	0.0519	1.8	K
SC-5.3	3.1E-04	0.0539	0.25	488	0.09	279	±2	22.7	0.78	0.0493	5.6	R2
SC-6.1	-1.0E-05	0.0532	0.14	1155	0.21	290	±3	21.7	0.92	0.0534	2.0	R1
SC-6.2	9.7E-03	0.1776	15.48	67	0.36	331	±5	19.5	3.41	0.0327	80.1	K 207 fail
SC-7.1	6.7E-05	0.0517	—	975	0.35	282	±3	22.4	0.94	0.0507	2.5	R2
SC-8.1	2.6E-05	0.0530	0.13	1516	0.02	286	±2	22.0	0.61	0.0527	1.5	R1
SC-9.1	6.3E-05	0.0528	0.10	1400	0.20	284	±2	22.2	0.61	0.0519	1.7	R2
SC-10.1	6.7E-04	0.0540	0.05	65	0.42	353	±5	18.0	2.11	0.0441	30.2	C1
SC-10.2	-1.2E-05	0.0527	0.08	1031	0.36	288	±2	21.9	0.64	0.0529	2.0	R1
SC-11.1	-5.5E-05	0.0514	—	79	0.48	372	±9	16.9	2.61	0.0522	19.0	C1 5% C2
SC-12.2	-2.3E-04	0.0520	—	46	0.54	361	±6	17.3	2.70	0.0554	31.5	C2
SC-13.1	5.8E-04	0.0523	—	97	0.68	308	±4	20.7	1.74	0.0437	24.4	MIX C1 + R1
SC-13.2	-8.2E-06	0.0514	—	543	0.10	295	±2	21.4	0.73	0.0516	3.7	R1
SC-14.1	-5.9E-05	0.0653	1.33	811	0.28	397	±6	15.5	1.53	0.0662	1.4	K C1
SC-14.2	-1.1E-05	0.0523	0.03	1870	0.31	288	±2	21.9	0.76	0.0525	1.2	R1
SC-14.3	9.1E-06	0.0525	0.05	813	0.27	290	±3	21.8	1.02	0.0524	2.9	R1
SC-15.1	-1.1E-04	0.0512	—	822	0.27	289	±2	21.8	0.70	0.0527	2.5	R2 is 14.3
SC-15.1 ... dup1	-2.0E-05	0.0548	0.19	100	0.46	337	±4	18.6	1.51	0.0551	14.9	C2
SC-15.2	4.2E-04	0.0603	0.94	608	0.10	318	±2	19.7	0.73	0.0542	3.8	K
SC-16.1	4.5E-05	0.0525	0.05	954	0.32	289	±3	21.8	0.89	0.0518	2.3	R1
SC-16.2	-1.4E-05	0.0513	—	141	0.56	363	±4	17.3	1.25	0.0515	11.6	C1
SC-17.1	-4.0E-04	0.1691	12.89	20	0.50	712	±63	7.4	5.35	0.1741	32.2	Co
SC-17.2 ... dup1	-5.4E-03	0.0502	—	19	0.72	367	±9	15.6	4.81	0.1228	24.9	C1
SC-17.3 ... dup1	-3.4E-03	0.0527	—	25	0.53	369	±9	16.0	4.07	0.0992	25.2	C1
SC-18.2 ... dup1	-3.6E-05	0.0527	0.05	848	0.14	298	±2	21.1	0.69	0.0532	2.3	R1
SC-18.3	-6.2E-05	0.0542	0.25	873	0.25	293	±2	21.4	0.73	0.0551	4.5	R1
SC-19.1	2.0E-03	0.0514	—	39	0.71	353	±11	18.5	4.90	0.0207	149.7	C2 b oz Th fail
SC-19.1	-5.5E-05	0.0539	—	42	0.70	376	±12	16.6	3.96	0.0547	36.5	C1, retake
SC-20.2	-7.1E-05	0.0541	0.28	444	0.16	279	±3	22.5	1.1	0.0552	3.4	R1 oz
SC-21.1	-1.9E-04	0.0512	—	122	0.53	364	±5	17.2	1.4	0.0540	7.5	C1 is 12
SC-21.2	2.9E-04	0.0565	0.33	147	0.37	365	±5	17.2	1.4	0.0523	7.8	C2 is 12
SC-22.1	-1.1E-04	0.0520	—	142	0.31	345	±4	18.2	1.4	0.0536	6.9	C2
SC-22.2	1.1E-04	0.0532	0.17	502	0.21	278	±3	22.7	1.0	0.0516	4.2	R2
SC-23.1	-1.2E-04	0.0526	—	120	0.80	362	±5	17.3	1.4	0.0544	7.7	C2
SC-24.1	-1.0E-04	0.0557	0.25	221	0.47	359	±4	17.4	1.2	0.0573	3.9	C2
SC-24.2	-3.3E-05	0.0521	—	167	0.63	349	±4	18.0	1.3	0.0525	5.5	C1
SC-24.3	-2.0E-04	0.0548	0.15	182	0.57	353	±4	17.7	1.3	0.0577	6.7	C1
SC-24.4	2.3E-05	0.0528	0.11	724	0.23	284	±3	22.2	1.0	0.0525	2.2	R1
SC-25.1	3.1E-05	0.0562	0.52	229	0.38	287	±4	21.9	1.3	0.0557	6.2	R1 > C2 oz
SC-26.1	4.8E-05	0.0545	0.31	578	0.12	283	±3	22.2	1.0	0.0538	2.7	R1 oz
SC-26.2	2.6E-04	0.0560	0.29	87	0.56	359	±5	17.5	1.6	0.0522	10.8	C1 > C2 oz
SC-27.1	-3.7E-05	0.0518	—	130	0.77	371	±5	16.9	1.4	0.0523	7.7	C1 oz
SC-29.1	-1.2E-04	0.0547	0.20	124	0.46	332	±4	18.8	1.4	0.0565	6.9	R1 > C2 oz
SC-30.1	-4.2E-05	0.0545	0.18	148	0.41	330	±4	19.0	1.4	0.0551	8.2	C2
<b>Lighthouse Point Granite, Lighthouse Park, New Haven, Conn. [41°14'56.50"N, 72°54'14.23"W]</b>												
14A-1.1	7.7E-4	0.0567	0.57	241	1.19	290	2	21.9	1.00	0.0454	12.0	oz c2
14A-2.1	5.3E-4	0.0832	0.49	111	0.31	1175	11	5.0	1.03	0.0756	4.6	C0 oz
14A-2.2	3.6E-4	0.0806	0.32	123	0.31	1146	12	5.16	1.2	0.0755	5.5	C0 oz
14A-3.1	4.9E-4	0.0680	1.75	80	0.70	369	9	16.8	2.97	0.0610	20.0	oz c2
14A-4.1	7.5E-4	0.0572	0.64	277	1.51	289	4	22.0	1.40	0.0461	12.2	oz c2
14A-5.1	1.5E-4	0.0535	0.21	2518	0.20	277	2	22.8	0.70	0.0513	1.8	oz r1
14A-6.1	1.4E-3	0.0656	1.69	170	0.91	286	5	22.2	2.25	0.0455	21.5	sz oz c
14A-7.1	2.4E-3	0.0686	2.07	154	1.47	282	4	22.9	1.97	0.0318	32.5	sz oz c2
14A-7.2	5.6E-4	0.0643	1.50	134	1.12	297	4	21.1	1.74	0.0562	14.0	sz c2
14A-9.1	8.8E-4	0.0586	0.78	270	1.23	301	2	21.1	0.94	0.0456	10.7	sz oz c2

(continued on next page)

**Table 1** (continued)

Sample <sup>a</sup> (location)	Measured $^{204}\text{Pb}/^{206}\text{Pb}$	Measured $^{207}\text{Pb}/^{206}\text{Pb}$	% Common $^{206}\text{Pb}$	U (ppm)	Th/U	$^{206}\text{Pb}^{\text{b}}/^{238}\text{U}$ (Ma)	Err <sup>c</sup> (Ma)	$^{238}\text{U}^{\text{d}}/^{206}\text{Pb}$	Err <sup>c</sup> (%)	$^{207}\text{Pb}^{\text{d}}/^{206}\text{Pb}$	Err <sup>c</sup> (%)	Notes <sup>e</sup>
14A-10.1	4.6E-4	0.0605	1.02	247	1.55	299	2	21.0	1.00	0.0539	9.4	oz c2
14A-10.2	4.1E-5	0.0530	0.07	2209	0.04	303	2	20.80	0.7	0.0524	1.8	oz r1
14A-11.1	1.6E-3	0.0668	0.83	63	0.62	605	9	10.4	1.88	0.0424	30.7	C0 sz oz 207f
14A-12.1	1.0E-3	0.0631	1.33	168	1.29	305	3	20.7	1.29	0.0481	16.6	oz c2
14A-13.1	7.6E-4	0.0607	1.07	276	1.53	289	2	21.8	0.96	0.0495	10.2	sz oz c
14A-13.2	1.1E-4	0.0590	0.81	237	1.18	307	2	20.4	1.02	0.0574	9.3	sz oz c
14A-13.3	6.6E-4	0.0668	1.80	186	1.06	300	3	20.8	1.26	0.0571	12.9	sz oz r
14A-13.4	1.3E-3	0.0700	2.24	239	1.21	285	5	22.2	3.16	0.0510	45.8	sz oz c
14A-13.5	7.4E-4	0.0588	0.83	232	1.05	293	2	21.6	2.67	0.0480	42.8	sz oz r
14A-13.6	1.6E-3	0.0722	2.49	155	1.11	292	3	21.7	3.81	0.0484	61.8	sz oz r
14A-15.1	4.2E-5	0.0809	—	154	0.70	1241	11	4.7	0.93	0.0803	2.7	C0 oz
14A-16.1	-4.9E-4	0.0545	0.28	216	1.01	298	7	20.9	2.59	0.0616	9.5	oz C1
14A-17.1	-3.2E-4	0.0603	1.01	137	1.08	294	3	21.1	1.52	0.0649	14.8	oz C2
14A-18.1	5.5E-4	0.0594	0.91	162	1.49	293	6	21.6	2.42	0.0513	16.0	sz c
14A-18.2	1.0E-4	0.0536	0.19	1481	0.02	288	4	21.9	1.42	0.0521	2.0	oz c
14A-19.1R	9.2E-5	0.0537	0.16	240	1.26	305	2	20.7	0.89	0.0524	7.8	sz oz c
14A-19.2	-1.1E-4	0.0593	0.85	239	0.86	306	2	20.4	0.95	0.0609	7.7	sz oz r
14A-21.2	-2.1E-4	0.0582	0.78	219	0.94	284	4	21.94	1.7	0.0612	14.6	oz c2
14A-23.1	1.8E-4	0.0652	1.18	388	0.09	439	8	14.06	1.9	0.0626	5.0	sz oz c
14A-23.2	4.3E-4	0.0559	0.48	250	0.77	287	5	22.04	1.9	0.0495	15.8	sz oz c
14A-23.3	7.8E-4	0.0581	0.76	217	0.90	284	3	22.33	1.5	0.0465	19.7	sz oz r
14A-23.4	7.4E-4	0.0594	0.95	238	0.87	276	4	22.9	2.86	0.0485	39.8	sz oz r
14A-24.1	5.4E-3	0.1298	8.75	191	1.46	550	6	11.34	1.4	0.0498	17.9	C0 oz c2
14A-26.1	1.7E-4	0.0546	0.35	2116	0.18	277	2	22.78	0.7	0.0522	1.9	oz r1
14A-26.2	7.5E-5	0.0615	0.12	191	0.68	624	6	9.85	1.1	0.0604	7.2	C0 oz c2
14A-27.1	5.7E-4	0.0584	0.79	422	0.98	286	2	22.08	1.0	0.0500	9.1	oz c2
14A-28.2	6.4E-5	0.0532	0.15	2491	0.03	286	3	22.07	1.1	0.0523	1.6	oz r1
14A-30.1	7.6E-5	0.0529	0.09	2124	0.03	292	3	21.57	1.0	0.0518	1.8	oz r1
14A-31.1	8.4E-4	0.0755	2.90	103	1.02	293	3	21.18	2.3	0.0634	25.9	oz c1
14A-32.1	1.6E-3	0.0662	1.74	119	1.06	296	3	21.57	2.0	0.0426	32.8	sz oz r
14A-33.1	6.6E-3	0.1592	13.32	419	0.97	297	3	20.91	2.3	0.0637	26.9	sz c
14A-34.1	6.9E-3	0.1554	12.91	423	1.31	278	3	22.6	1.6	0.0544	15.6	oz r

<sup>a</sup> All samples analyzed on the Korean Basic Science Institute ion microprobe (SHRIMP-IIe/MC) in July 2010. ra, grain reanalyzed.

<sup>b</sup>  $^{206}\text{Pb}/^{238}\text{U}$  ages corrected for common Pb using the  $^{207}\text{Pb}$ -correction method. Decay constants from Steiger and Jäger (1977).

<sup>c</sup> 1-Sigma errors.

<sup>d</sup> Radiogenic ratios, corrected for common Pb using the  $^{204}\text{Pb}$ -correction method, based on the Stacey and Kramers (1975) model.

<sup>e</sup> Notes on internal zircon structure: C1, inner core; C2, outer core; C0, inherited core; c, undefined core; R1 inner rim; R2, outer rim; r, undefined or single rim; sz, sector zoned region; oz oscillatory zoned region; <, >, +, spot overlapped two zones, greater than, less than, or equally; K, spot intersected a crack in the zircon grain; fail, analysis for isotope failed.

Zircon in the NPG is clear and colorless or pale yellow to orange. Most abundant are the clear grains that occur in several shapes: 1) grains 80–150  $\mu\text{m}$  long, with aspect ratios of two-to-one; 2) stubby subhedral ovoid grains 200  $\mu\text{m}$  long and up to 100  $\mu\text{m}$  wide; 3) longer euhedral to subhedral grains up to 300  $\mu\text{m}$  with aspect ratios of 3:1 (Fig. 3A–C); and 4) strongly acicular euhedral grains up to 350  $\mu\text{m}$  long and with aspect ratios of 4:1 to 6:1. Pale yellow to orange grains are also present: they may be euhedral to subhedral, translucent and contain  $\mu\text{m}$ -size red inclusions in transmitted light that give the grains their orange color. A smaller subset of these grains contain cracks that are stained orange (see also Zartman and Hermes, 1987). BSE and CL imaging shows oscillatory zoning of cores of the grains to be ubiquitous. These grains contain two major structural divisions: a low U, moderately to highly luminescent core, and a U-rich, non-luminescent rim. The repeated oscillatory zoning, relatively high U concentrations, and Th/U ratios ( $>0.2$ ; Fig. 3) all suggest that these grains crystallized from a magmatic liquid.

#### 4.1.1. Zircon textures

Cores with relatively low U concentrations are characterized by conspicuous fine oscillatory zoning and rarer sector zoning. Many grains show multiple bands of concentric oscillatory zoning. Boundaries between these bands truncate oscillations of the band below. These truncations define disconformities and angular unconformities with as many as six such unconformities in some

grains (arrows, Fig. 3A). Irregular dissolution or resorption of (less luminescent) zircon into the magma truncated the original (magmatic) oscillatory zoning, whereas newly precipitated (highly luminescent) zircon from the magma preserved that partially dissolved surface under the overgrowth. For this study an inner core region “C1” is identified where two or more truncating overgrowths surround the inner core, and “C2” is assigned to the regions outside of two or more interior zones (Table 1). Where one or no unconformities are exposed at the depth of intersection with the polished surface, an interpretation of outer “C2” core is assigned.

All cores are surrounded by inner and outer mantles. The inner mantles or inner rims (R1) are composed of oscillating sets of 2–20  $\mu\text{m}$ -wide bands of pale and dark gray zircon (in BSE imaging) of moderate to high U content. These outline euhedral shapes (Fig. 3), suggesting that they crystallized from a magmatic liquid. Exploratory EMPA analysis shows that this oscillatory zoning correlates with relatively high and low concentrations of Fe and Y, respectively. In some grains, these broadly zoned bands alternate with irregular bands 10–20  $\mu\text{m}$  wide composed of 1–5  $\mu\text{m}$  grains of zircon interspersed with 1–2  $\mu\text{m}$  grains of  $\text{YPO}_3$ , an FeAl-silicate, and  $\text{UO}_2$  (Fig. 3B). These inclusion-rich bands show no internal structure, whereas the inner and outer walls of these bands truncate zoning in both adjacent bands (Fig. 3B). These R1 rims are overgrown and embayed by subsequent R2 bands (Fig. 3). An interesting feature of this R2 zircon is that it also embays the low-U, CL luminescent cores and may completely replace the core regions

of some grains. In this case, rimming and replacement zircon are of the same generation. The irregular truncations of oscillatory bands under successive stages of overgrowth demonstrate that dissolution of older material preceded each phase of overgrowth.

#### 4.1.2. Isotopic results

The results of the SHRIMP analysis are given in Table 1 and compared in Fig. 3D. Of 70 initial analyses, 48 analyses are regarded as reliable. Of these, 45 yield concordant or nearly concordant ages; three analyses of young rims contain high common  $^{206}\text{Pb}$  (Fig. 3D). Some analyses were discarded either because the correlation of the five analytical iterations per analysis failed or because the analysis spot intersected a modern crack, allowing contamination. Some of these discarded analyses were on locations showing very complicated internal structures (e.g. Fig. 3B). The vast majority of grains are early Permian; 36 grains yield an age of  $283 \pm 1.6$  Ma (Fig. 3D). Regression of inner and outer cores separately yields the same age. Both sets of cores have similar Th/U (Fig. 3E, Table 1).

The age of crystallization of the orange and clear rims is poorly defined by these results. Many analyses of replacement zircon were rejected because the high density of healed cracks in this material could not be avoided (Fig. 3B). This may have been associated with U gain or Pb loss during recrystallization (see below). The ages of four acceptable rims range between ~272 and ~288 Ma (Table 1).

The ages of two younger rims agree with two whole-grain TIMS ages of monazite separates of ~273 Ma (Zartman and Hermes, 1987), suggesting that a younger, and perhaps sub-solidus but still hot, recrystallization event occurred at this time. Four other grains were identified that contain inherited cores surrounded by younger Permian overgrowths. The results (replicated in grains NP-22 and NP-48, Table 1) are nearly concordant and give Neoproterozoic ages (e.g. Fig. 3C), whereas the analytical spots on two other grain cores overlapped slightly with overgrowths and gave younger ages that still reflect a Neoproterozoic inheritance.

Some Neoproterozoic cores contain cracks healed by zircon: these are never present in the Permian grains or overgrowths. For example, in grain NP48 (Table 1) a crack breaks the core of the grain but not the rim. Rather, it is healed with non-luminescent zircon similar to the surrounding rim (arrow, Fig. 3C). The rims are Permian, so the grain could have been broken at any time between ~600 and 290 Ma. However, repeated healing of fractures by Permian zircon in multiply fractured grains in other samples (see below) indicates an Alleghanian fracturing event.

#### 4.2. Potter Hill Gneiss

The Potter Hill Gneiss of Feininger (1964, 1965) is one of several gneisses assigned a Neoproterozoic age by Rodgers (1985). It is a

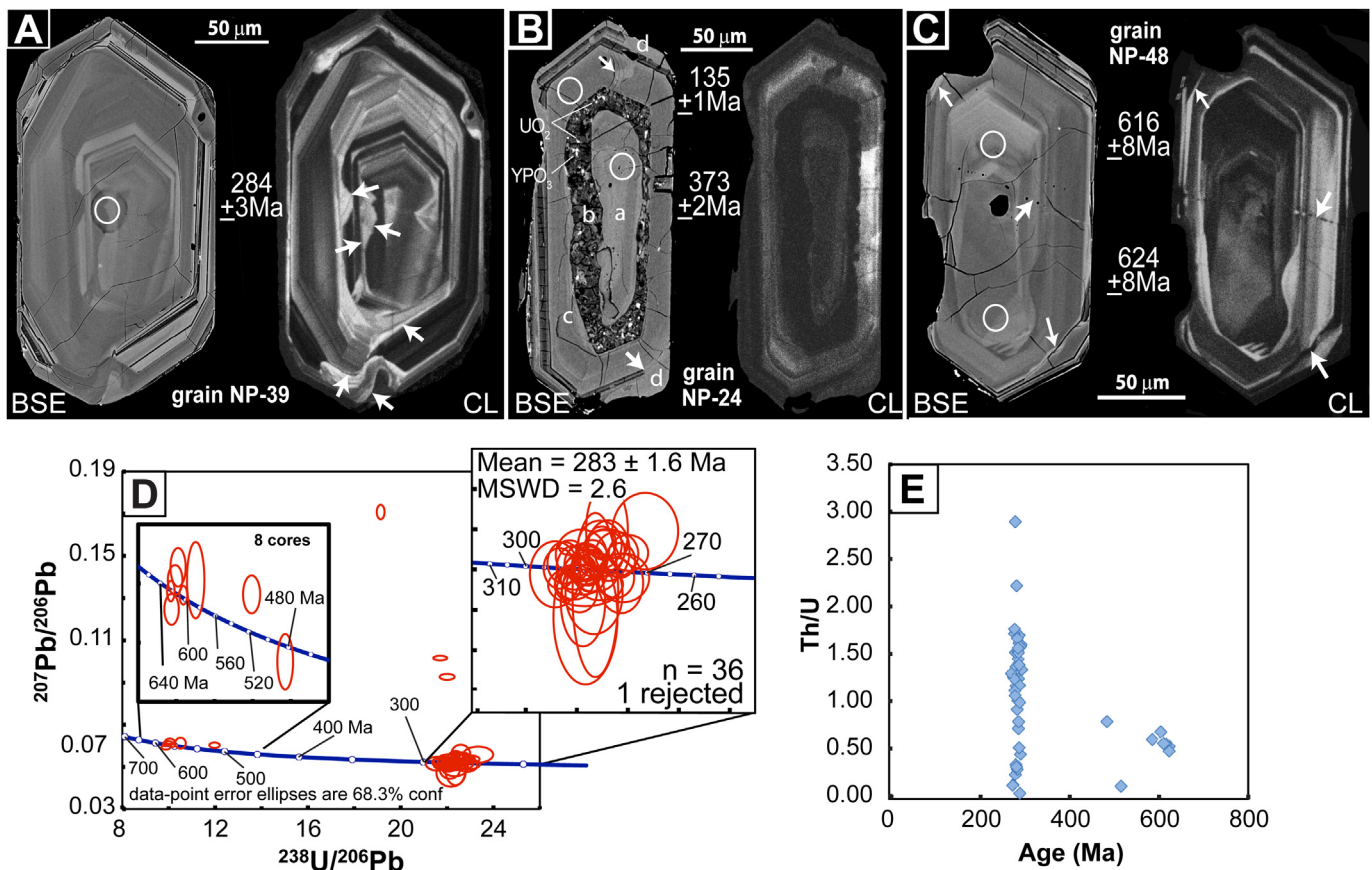


**Fig. 3.** Results of SEM and isotopic analyses of zircons from the Narragansett Pier Granite. Circles identify the locations and size of the analytical SHRIMP spot with ages given in Ma. A. Backscattered electron (BSE) and cathodoluminescence (CL) images of a Permian grain showing as many as 6 generations of dissolution and overgrowth events (white arrows, CL image). Arrows point to the 'unconformable' boundaries between growth zones. B. BSE and CL images of a relatively large euhedral grain showing a complicated growth pattern. The grain is U-rich, and so relatively bright in BSE but not luminescent in CL. An inner core euhedral core (a) is truncated by dark granular-appearance zone (b) containing bright, disseminated,  $\mu\text{m}$ -size grains of UO<sub>2</sub> and YPO<sub>3</sub>. This zone is mantled by a subhedral multi-layered zone (c), followed by a rim of relatively bright zircon that embays the SE corner (d) and invades the NE corner of the grain (arrows). C. BSE and CL images of a subhedral, oscillatory zoned, Neoproterozoic zircon grain, showing cracks healed by U-rich zircon (bright in BSE and dark in CL). D. A Tera-Wasserburg diagram summarizing the results of isotopic analyses (Table 1). E. Diagram comparing the very large range of Th/U of the Permian grains with the smaller range of Proterozoic grains.

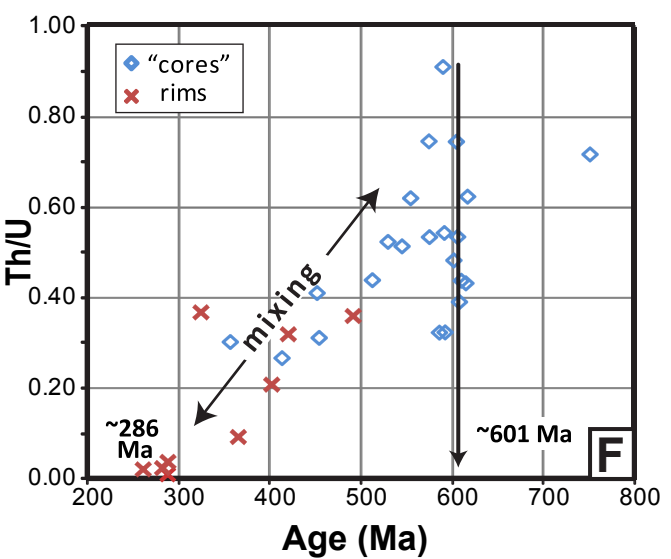
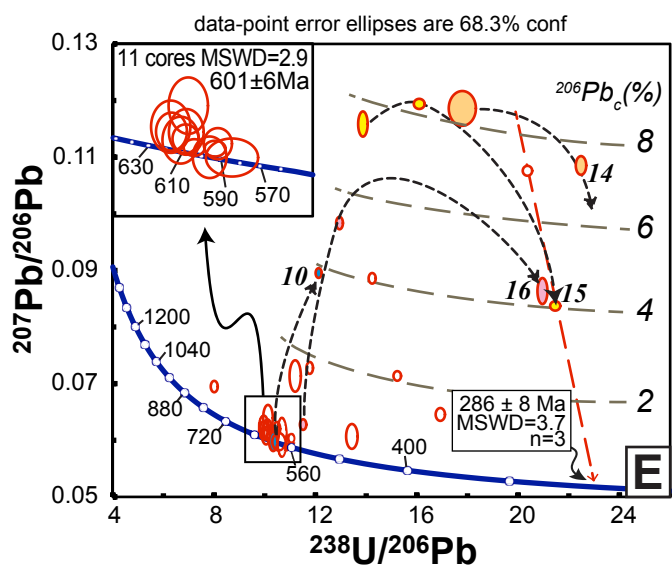
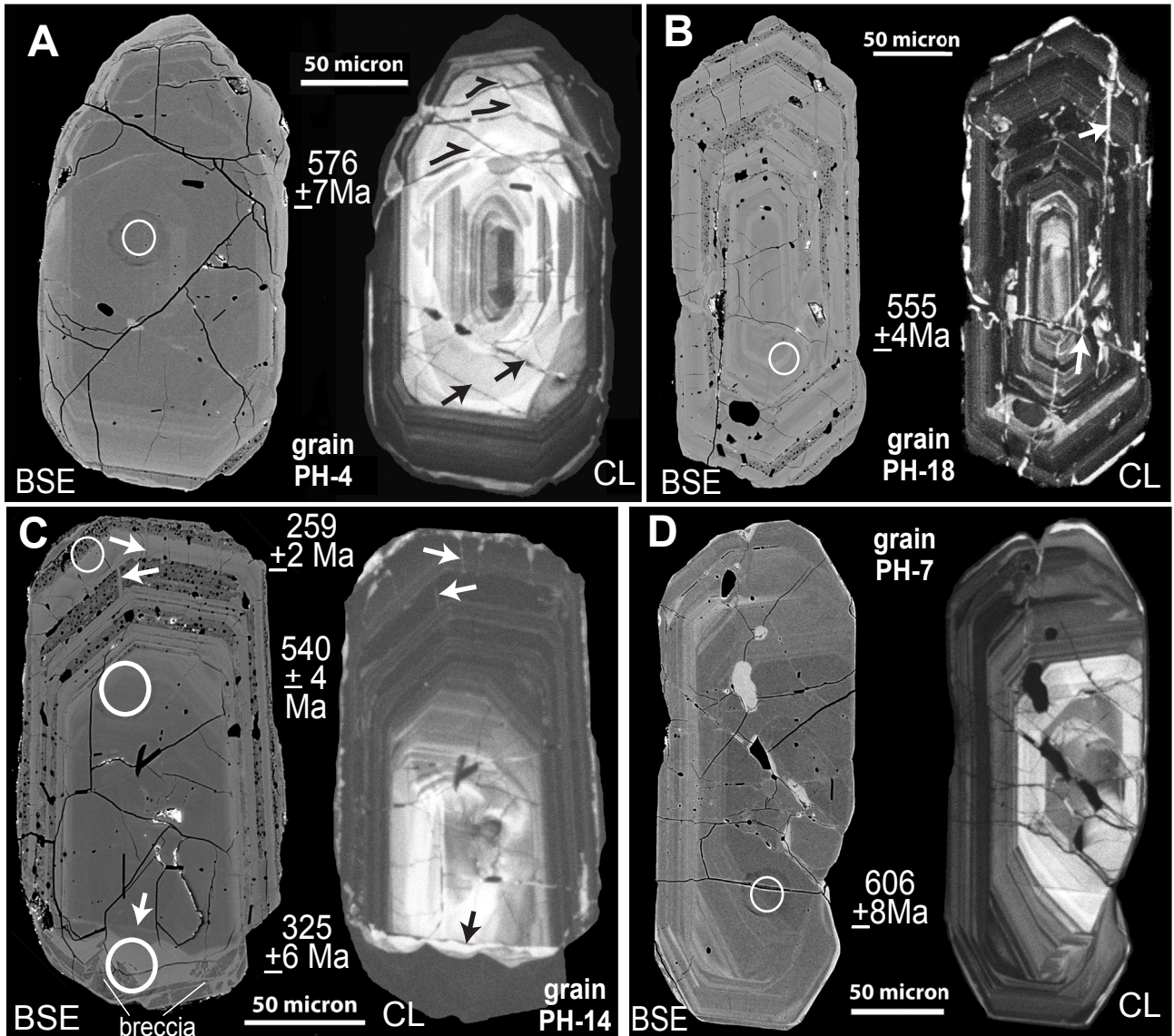


**Fig. 4.** Results of SEM and isotopic analyses of zircons from the Potter Hill Granite. Circles identify the locations and approximate size of the analytical SHRIMP spot with ages given in Ma. Figs A–D are BSE and CL image pairs of zircon grains showing a bright (in CL), oscillatory zoned, Neoproterozoic cores with a dark (in CL) Permian rim. The cores are fractured

pale pinkish-gray, weakly foliated granite with lenses of finer grained alaskite and porphyry, and xenoliths and blocks of biotite schist and Hope Valley alaskite (Loughlin, 1912; Martin, 1925; Foye, 1949; Goldsmith, 1985). Our sample was collected from a road cut on the eastbound ramp of exit 92 off I95 in North Stonington.

#### 4.2.1. Zircon textures

The zircon population in this sample of the Potter Hill granofels is dominated by translucent grains stained orange, but smaller clear grains form a significant sub-group and large mottled milky-tan grains are also present. Most grains contain luminescent cores with fine concentric, oscillatory, and rarely also sector, zoning (Fig. 4). U concentrations range between about 100 and 500 ppm. Truncations of some oscillatory zones by successive bands of overgrowths (also oscillatory) produce ‘unconformities,’ similar to grains in the Narragansett Pier granite. Over 90% of the grains contain cores that are fractured and healed by luminescent and non-luminescent zircon ‘veins’ that connect to overgrowths (Fig. 4). Some fractures show minor displacement (Fig. 4A) and other grains are broken fragments (arrows, Fig. 4C). These cores are commonly mantled by thin to thick orange-stained overgrowths producing subhedral composite grains typically 200–300 µm in length with aspect ratios of 3:1 to 4:1. Thin outer rims truncate oscillatory zoning in underlying bands, showing that the final stages of growth were preceded by a dissolution event.

The orange color of most grains derives from multiple oscillatory bands of two types. Bands rich in Fe that contain in 1–2 µm silicate inclusions (Fe–Al–Si silicates > epidote > quartz > K-feldspar) alternate with inclusion-free bands richer in U and brighter in BSE imaging (Fig. 4B, C). Zircon in these U-rich bands fill small veins that cut the Fe-rich bands. Even the U-rich overgrowths can be fractured as shown in grain 14, where a breccia at the broken end is cemented by a U-rich zircon (Fig. 4C). A complicated history of fracturing and healing is clearly demonstrated by these textures. The fact that even micrometer-size fragments of zircon are angular indicates that dissolution of these shards into a silicate liquid was minimal. These observations lead to the conclusion that the modest amount of zircon recrystallization in this sample occurred in the solid state, without the aid of a partial melt. Only the outermost rims of the grains embay the enclosed layers, consistent with dissolution into, and precipitation from, a magma.

#### 4.2.2. Isotopic results

Of the 37 SHRIMP sites analyzed, 31 are reliable and are reported in Table 1 and summarized in Fig. 4E. The Tera-Wasserburg concordia diagram shows a considerable dispersion of analyses, some with high concentrations of common lead ( $^{206}\text{Pb}_{\text{C}}$ ) resulting in highly discordant data. Grains 10, 14, 15, and 16 show a curious pattern of rising and falling concentrations of  $^{206}\text{Pb}_{\text{C}}$  with decreasing apparent age (Fig. 4E). A subset of 11 concordant analyses from unfractured, low U, luminescent cores of composite grains yields an age of ~600 Ma (Fig. 4E). The analyses of three relatively pure rims yield an age of  $286 \pm 8$  Ma, an age that overlaps within uncertainty with the age of three concordant whole-grain monazite U–Pb TIMS ages of  $279 \pm 2$  Ma (Gromet et al., 1998), but these ages undoubtedly average growth zones.

The spot size of the remaining analyses was too large to isolate either core or overgrowths, and so reflect mixtures. Overgrowth material contains much more U and more  $^{206}\text{Pb}_{\text{C}}$  (Table 1; Fig. 4E) and apparently lower Th/U ratios (Fig. 4F). The effect of overlap with overgrowth material is to increase the  $^{206}\text{Pb}_{\text{C}}$  content of the bulk analysis and lower the apparent age. Multiple analyses across single grains that overlapped both Proterozoic cores and Permian overgrowths and fractures produced arcuate paths of rising and then falling  $^{206}\text{Pb}_{\text{C}}$  concentration with decreasing age (curves, Fig. 4E). With increasing purity of the overgrowth component, the  $^{206}\text{Pb}_{\text{C}}$  concentration falls to ~4%. Apparently the interface between the dissolving Neoproterozoic cores and the replacing Permian overgrowths resulted in high concentrations of  $^{206}\text{Pb}_{\text{C}}$ . The mixing of these two components is further demonstrated by the negative correlation of the Th/U ratio with apparent age (Fig. 4F). The oscillatory zoning and high Th/U ratios of the cores suggest that the original grains crystallized from a magma in the late Proterozoic. The overgrowth and fracture-filling zircon are generally unzoned, and the mixing line of Fig. 4F suggests that they have a low Th/U ratio.

#### 4.3. Stony Creek Granite

The Stony Creek Granite is a pink to red, medium to coarse-grained, migmatitic granite. Biotite-rich schlieren or strands (~1–10 mm thick) are characteristic, and the moderate preferred orientation of the biotite gives the rock a wispy gneissosity. Earlier studies (e.g. Percival, 1842; Kemp, 1899; Barrell and Loughlin, 1910; Dale and Gregory, 1911; Foye, 1949, see Rodgers et al., 1959) included the Stony Creek granite within a continuous band of undifferentiated granitic rock exposed along Long Island Sound. Rodgers (1985) accepted more recent mapping (Mikami and Digman, 1957; Bernold, 1962; Sanders, 1968) and dating (Hills and Dasch, 1972) that revealed this granite intruded a structurally higher quartzite (McLellan and Stockman, 1985; Stockman and McLellan, 1987; McLellan et al., 1993). Other phases of granitic rock include finer grained dikes, pegmatites with both sharp and diffuse boundaries, and migmatites that are pervasive throughout the area (McLellan and Stockman, 1985). Our sample was collected from a massive granite that occurs well removed from local pegmatites and migmatites in the still active Stony Creek Quarry of Dale and Gregory (1911).

#### 4.3.1. Zircon textures

Most zircon grains in our sample of Stony Creek granite are clear, colorless, and inclusion-free; they are 150–350 µm long, with aspect ratios of 2:1 to 3:1. A small proportion of grains (~10%) contain small micron-scale opaque inclusions. All grains examined are composite. They contain partially resorbed, oscillatory-zoned cores with U concentrations of less than 150 ppm and zoned mantles that contain between 400 and 1800 ppm U. Most oscillatory zoning in inner cores (C1, Table 1) is truncated by at least one band of zircon overgrowth that is also luminescent and oscillatory zoned (C2; Fig. 5A, Table 1).

These luminescent cores are universally mantled by U-rich overgrowths that are dark in CL but also show oscillatory zoning in BSE imaging. These rims always truncate the luminescent bands in

(arrows) and filled by younger zircon contiguous with the zircon in the rim. In A the upper fractures show displacement as micro-faults (thrust symbols). The analytical spot in B probably overlaps on the left with a Permian zircon crack filling. C shows that the lower half of the grain is actually dismembered and removed. The smooth boundary between the fractured core and the bright overgrowth (black arrow in CL) show a U-poor bunting-like overgrowth followed by a much thicker U-rich (dark) overgrowth. Even the overgrowth is brecciated (BSE). D. An anhedral grain showing that a modern crack does not appear to contaminate a Neoproterozoic core, whereas other healed fractures probably would have done so. E. A Tera-Wasserburg diagram showing that the analyses of the Neoproterozoic cores are largely concordant, whereas the analyses of the rims show considerable scatter caused by common lead ( $^{206}\text{Pb}_{\text{C}}$ ) up to 8% (Table 1). Multiple analyses of grains 10, 14, 15, and 16 show a progressive rise and fall in  $^{206}\text{Pb}_{\text{C}}$  approaching an age of 286 Ma (dashed arcuate arrows join analyses). F. A comparison of Th/U with age showing the data define a crude mixing line between Neoproterozoic cores with variable Th/U and Permian overgrowths with relatively low Th/U.

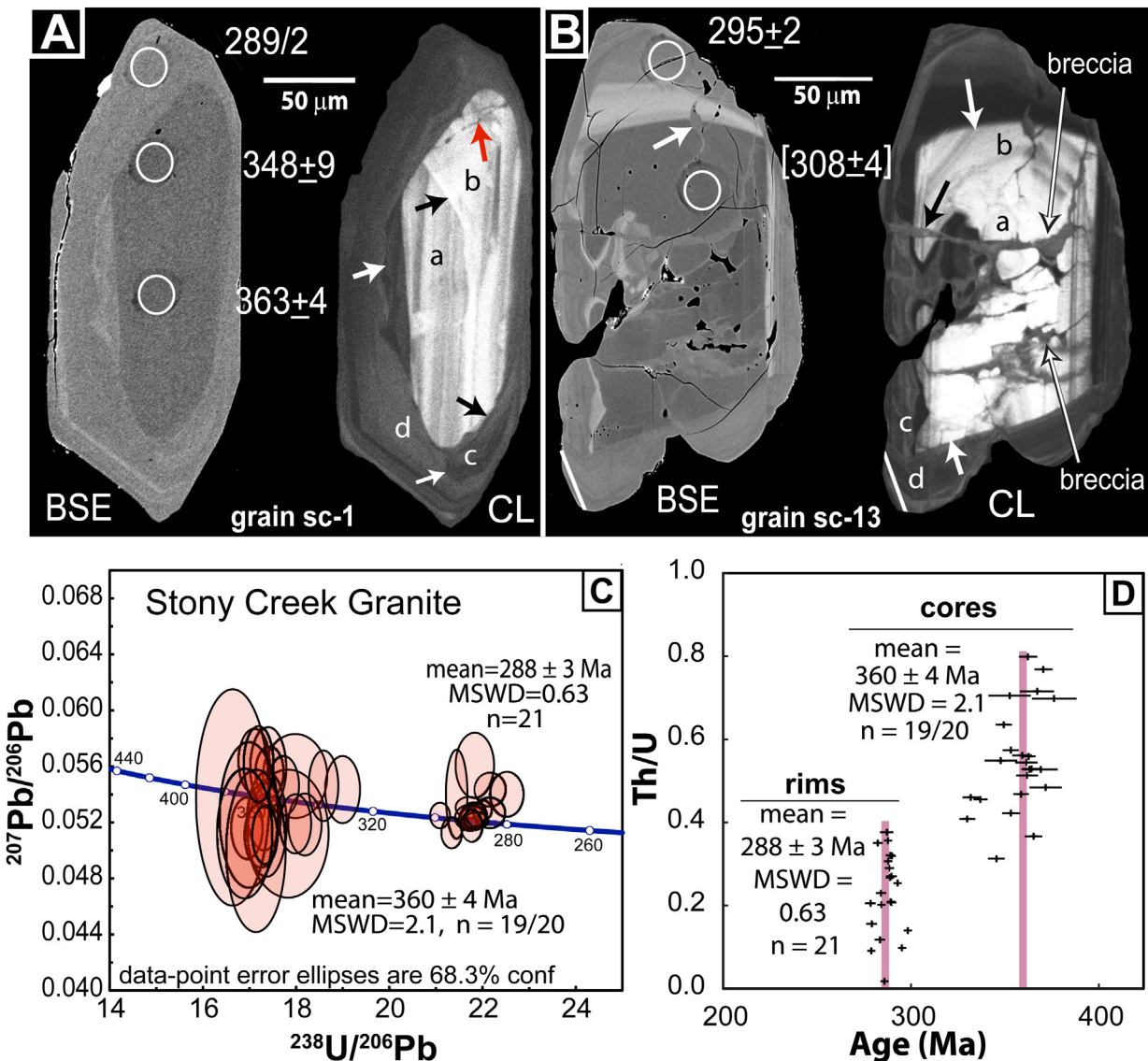


**Fig. 5.** Results of SEM and isotopic analyses of zircons from the Stony Creek Granite. Circles identify the locations and approximate size of the analytical SHRIMP spot, with ages given in Ma. **A.** A typical zircon grain showing oscillatory zoning in an anhedral luminescent Devonian core and a less luminescent euhedral Permian rim. The core contains two zones, a and b, separated by a dissolution-overgrowth (unconformable) boundary (black arrow). Zone b is fractured and healed by non-luminescent zircon (red arrow). Permian overgrowth truncates all zoning in the core and shows at least one dissolution-precipitation boundary (white arrows) separating an inner rim c from an outer rim d. **B.** An intensely broken zircon with a brecciated luminescent Devonian fragment in the core and a less luminescent Permian overgrowth. The core shows sharp truncations of the oscillatory zoning at the top and bottom (white arrows) where the core was broken before being overgrown. The Early Permian rim shows an abrupt increase in brightness in the BSE image, caused by a higher U, Th, and common Pb concentrations in the early overgrowth. At least two zones (labeled c and d in CL image) are present and zircon from both generations fills and heals fractures in the core, and in overgrowth zone c (black arrows). **C.** A Tera-Wasserburg diagram showing the distribution of analyses. **D.** A diagram comparing the Th/U with age, showing the Devonian cores have a generally higher ratio than the Permian overgrowths. (For interpretation of the references to color in this figure legend, the reader is referred to the web version of this article.)

the core, as well as the internal unconformities (e.g. Fig 5A). In some grains truncations are so abrupt that the core appears to be a dismembered fragment of a larger grain. For example, the white arrows in Fig. 5B identify fractured surfaces that truncate zircon cores. Most rims show multiple stages of overgrowths also separated by ‘unconformities.’ The external shapes of many grains are subhedral because overgrowths themselves may be slightly resorbed and their internal banding truncated at the outer grain boundary.

In addition to a history of multiple crystallization and resorption events, some grains also display a complicated history of fracturing. The fractures are visible especially in CL imaging by either brighter or darker luminescent zircon ‘veins’ that heal the fractured host zircon. The luminescence of the 1–5 µm wide fracture-filling zircon

typically corresponds to that of the innermost overgrowth. However, multiple cross-cutting fractures are present in some grains (Fig. 5B). In this case, the later healed fractures cut earlier healed fractures, suggesting that the cataclasis was a progressive event.

#### 4.3.2. Isotopic results

In spite of the strong textual evidence for multiple crystallization events, the SHRIMP analytical data are not able to resolve all age differences. The data cluster closely on a Tera-Wasserburg Concordia diagram where most of the uncorrected data lie on Concordia (Fig. 5C). The weighted mean of 19 of 20 analyses of cores yields an age of  $360 \pm 4$  Ma, while all 21 analyses of rims yield a weighted mean age of  $288 \pm 3$  Ma. The analytical data for cores and rims show a difference in their Th/U ratios (Fig. 5D), where the rims

**Table 2**

Major, trace element and isotopic compositions Stony Creek granite.

	SC-105	SC-205	SC-505	SC-705	SC-105	SC-205	SC-505	SC-705
<b>SiO<sub>2</sub></b>	71.851	69.490	75.390	72.592	<b>Rb</b>	190.5	153.5	169.5
<b>TiO<sub>2</sub></b>	0.1	0.317	0.203	0.316	<b>Sr</b>	362	334	109.5
<b>Al<sub>2</sub>O<sub>3</sub></b>	15.265	15.36	13.061	14.182	<b>Ba</b>	1490	1135	497
<b>FeO</b>	1.242	2.951	2.089	2.111	<b>La</b>	87.1	184.5	131
<b>MnO</b>	0.01	0.019	0.069	0.022	<b>Ce</b>	162	349	273
<b>MgO</b>	0.192	0.481	0.185	0.53	<b>Pr</b>	17.75	38.5	33.2
<b>CaO</b>	1.225	1.887	1.046	1.453	<b>Nd</b>	62.64	122.10	117
<b>Na<sub>2</sub>O</b>	3.158	3.757	3.162	2.983	<b>Sm</b>	9.09	17.82	23.9
<b>K<sub>2</sub>O</b>	6.598	4.603	4.493	5.41	<b>Eu</b>	1.66	2.22	1.7
<b>P<sub>2</sub>O<sub>5</sub></b>	0.04	0.141	0.084	0.08	<b>Gd</b>	6.43	14.35	22
<b>LOI</b>	0.48	0.57	0.34	0.47	<b>Tb</b>	0.54	1.18	3.03
Total	100.16	99.57	100.12	100.15	<b>Dy</b>	1.58	3.34	14.2
					<b>Ho</b>	0.21	0.48	2.42
<sup>143</sup> Nd/ <sup>144</sup> Nd	0.512019	0.512003		0.512077	<b>Er</b>	0.54	1.36	7.2
<sup>143</sup> Nd/ <sup>144</sup> Nd <sub>i</sub>	0.511858	0.511841		0.511890	<b>Tm</b>	0.03	0.12	1.16
$\varepsilon_{\text{Nd0}}$	-12.1	-12.4		-10.9	<b>Yb</b>	0.23	0.79	8.57
$\varepsilon_{\text{Nd(360 Ma)}}$	-7.1	-7.4		-6.6	<b>Lu</b>	0.03	0.12	1.36
$T_{\text{DM}}$	1369	1393		1466	<b>Zr</b>	103	313	272
<sup>208</sup> Pb/ <sup>204</sup> Pb	39.911	41.491		40.269	<b>Y</b>	5.8	12.6	62.6
<sup>207</sup> Pb/ <sup>204</sup> Pb	15.679	15.687		15.672	<b>Nb</b>	3.7	7.9	9.9
<sup>206</sup> Pb/ <sup>204</sup> Pb	18.277	18.294		18.430				10.4
Latitude N	41.34196	41.34395	41.26607	41.48334				
Longitude W	71.94478	71.93020	72.72556	72.08044				

$T_{\text{DM}}$  calculated using a linear evolution for a mantle separated from the CHUR at 4.55 Ga and having a present day Epsilon value of +10 (Gradstein et al., 2004).

have lower Th/U ratios due to the rise in U concentrations faster than the Th concentrations. To explore the possibility that the multiple generations of core and rim might have statistically different ages, as was found to be the case with sphene (Wintsch et al., 2005), the inner and outer core data and rim data were reduced separately. The weighted mean averages of the pairs of core and rim data overlap at the 2-sigma level, so that only a single age of the core and rim can be identified. We conclude that the Stony Creek granite began to crystallize in the latest Devonian and that an important overgrowth event occurred at about 288 Ma, followed by a major fracturing and dissolution event. Four inherited cores were found, but only two of these gave near concordant isotopic results. These grains display oscillatory zoning, have low to moderate U and Th concentrations, and yield ages of ~700 and ~1450 Ma (Table 1).

#### 4.3.3. Whole-rock chemical results

With the unexpected results of a Late Devonian age, we analyzed several samples of Stony Creek granite for major, trace element, and isotopic compositions (Table 2). Major element concentrations show that these rocks are true granites, and norm calculations show they are slightly peraluminous. Isotopic compositions indicate that they were derived from evolved sources.

#### 4.4. Light House Gneiss

The Light House Gneiss (Rodgers, 1985) is a massive, pink to buff to tan weathering granite. This rock was collected to ascertain its age and zircon inheritance at the western limit of rocks of potential peri-Gondwanan affinity. Foliation is generally only weakly developed. Structures that do exist include cross-cutting pegmatites (with diffuse boundaries), aplites, and quartz veins (Ward, 1909; Mikami and Digman, 1957).

#### 4.4.1. Zircon textures

Two types of zircon grains were recovered from the Light House Gneiss: elongate grains with prismatic oscillatory zoning, and equant grains with concentric oscillatory and sector zoning.

Prismatic grains are 75–200 µm long with aspect ratios of 2:1 to 3:1. They are composite grains generally containing U-poor, luminescent cores, some with oscillatory and sector zoning (Fig. 6A) and others overgrown by non-luminescent, U-rich rims (Fig. 6B; Table 1). The cores generally do not show the multiple resorption and overgrowth structures that are present in the other samples. In contrast, most U-rich rims show multiple bands of overgrowths, some separated by only minor resorption events producing low angle 'disconformities.' Oscillatory zoning bands in the luminescent cores are truncated and some are strongly embayed by the U-rich overgrowths, again demonstrating that a strong resorption event preceded the crystallization of the overgrowth.

The second major type of grain is characterized by conspicuous concentric sector zoning (Fig. 6B). These grains make up about 10% of the zircon population and tend to be larger than the prismatic grains, up to 200 µm in diameter. They are strongly luminescent, containing relatively low concentrations of U and Th, but their Th/U completely overlap with this ratio in prismatic grains.

#### 4.4.2. Isotopic results

Although the textures of these grains vary greatly, the isotopic data cannot resolve any difference in the ages of these varieties. Most analyses cluster tightly in a Concordia diagram (Fig. 6C) and no relationship is apparent between Th/U and age (Fig. 6D). The weighted average of 30 cores is  $292 \pm 3$  Ma with an MSWD of 8.4. The weighted means of all subsets of the zoning types shown in Fig. 6 overlap with this age, in spite of the U-rich compositions of the rims (Table 1). We conclude that this age reflects the time of crystallization of the Light House magma. The lack of foliation in this rock suggests that this age places a lower limit on the age of important sub-solidus Alleghanian deformation in this western tip of the peri-Gondwanan wedge.

The zircon population also includes five grains with Proterozoic ages that demonstrate inheritance. Two grains yield ages of ~1200 Ma, an age confirmed by replicate analysis (grain 14A-2.1, Table 1). Two other grains give ages of ~600 Ma. One other grain (14A-24.1) with a rather high <sup>206</sup>Pb<sub>C</sub> content is probably also Proterozoic. The 600 Ma ages are similar to peri-Gondwanan rocks

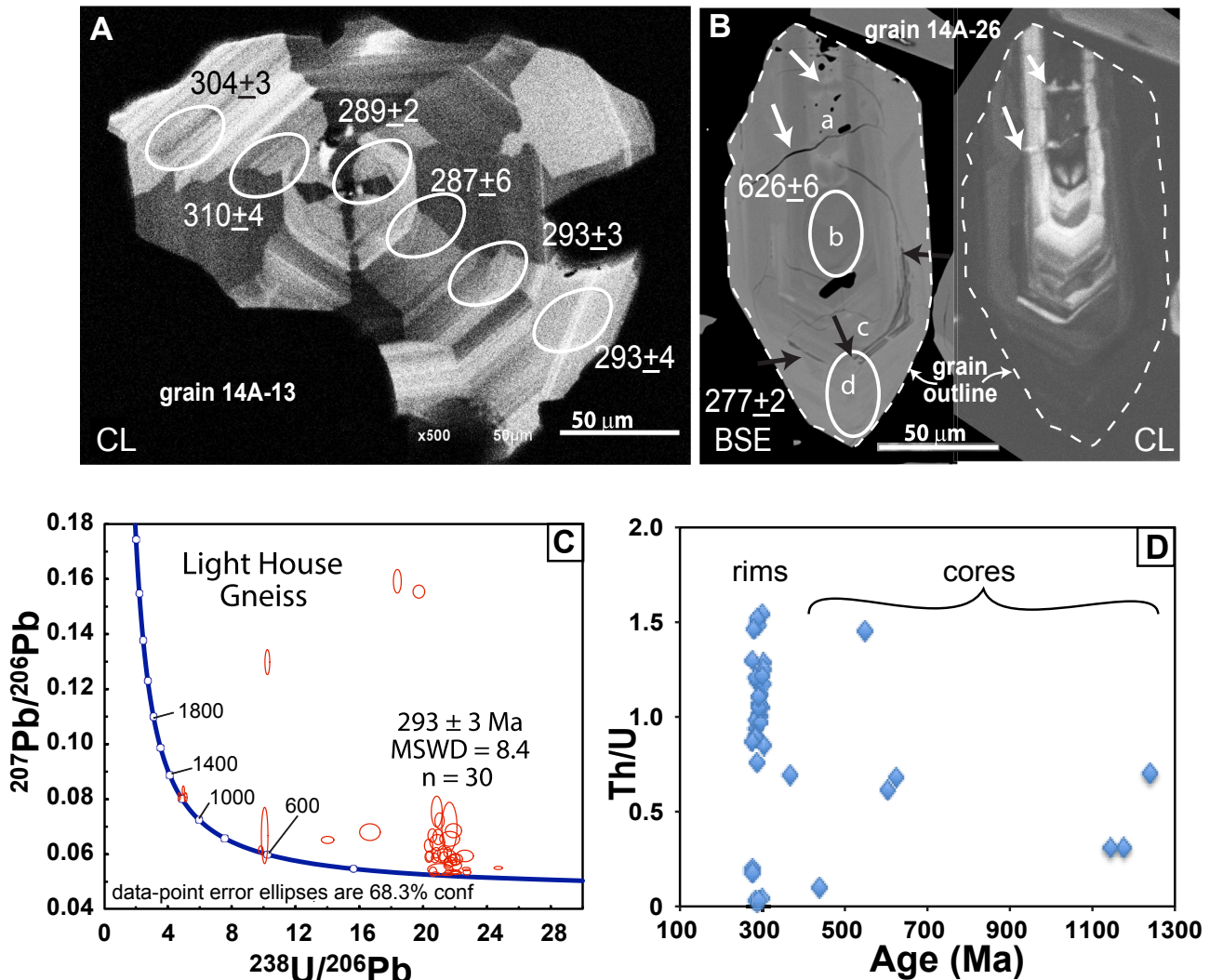


**Fig. 6.** Results of SEM and isotopic analyses of zircons from the Lighthouse Point Granite. Circles identify the locations and approximate size of the analytical SHRIMP spot, with ages given in Ma. **A.** An anhedral luminescent Permian zircon grain typical of those showing both oscillatory and sector zoning. **B.** A zircon grain typical of those with Neoproterozoic cores and Permian rims (outlined in white dashed line for clarity in the CL image). Fractures that cut the core but not the overgrowth are apparent (white arrows). The core probably contains 2 stages of growth (a and b) and the overgrowth shows at least one truncation surface (black arrows) separating the interior overgrowth (c) from an exterior rim (d). **C.** A Tera-Wasserburg diagram showing the distribution of analyses, many with large common Pb concentrations. **D.** The distribution of Th/U with age, showing the wide range of Th/U among the Permian grains.

present to the east, and the 1200 Ma grains are similar to Laurentian rocks present to the west. Together these inherited grains suggest that this magma is second cycle, derived from partial melting of lower crustal peri-Gondwanan rocks in the Permian.

#### 4.5. Summary of geochronology results

The isotopic results above show that the Narragansett Pier Granite and Light House Gneiss crystallized in the Early Permian, whereas the Stony Creek Granite crystallized in the latest Devonian. Neoproterozoic inheritance in the cores of some grains in each of these units suggests that they were derived by partial melting of peri-Gondwanan rocks. Neoproterozoic zircons in the Potter Hill granite-gneiss contain pervasive fracturing and minimal Permian overgrowths, showing that this unit is a Neoproterozoic granite, deformed and metamorphosed but not extensively melted in the Permian.

## 5. Discussion

The above isotopic results establish a common Permian age for the time of last crystallization of zircon in these four granitoids. However, inheritance is observed in all samples. The textures and intergrowths preserved within zircon cores identify brittle metamorphic processes that affected all four units now exposed along south coastal New England, as well as processes involving the crystallization of zircon from granitic magmas. These topics are discussed in more detail below.

### 5.1. Devonian magmatism

The U–Pb age of Stony Creek Granite is surprising in that it had previously been considered to be a Neoproterozoic rock with a Permian overprint (Rodgers, 1985). However, new SHRIMP data indicate a Late Devonian ( $360 \pm 4$  Ma) crystallization age. This age is similar to the age of some granites and rhyolites in Rhode Island

and eastern Massachusetts (e.g. [Hermes and Zartman, 1985](#); [Thompson and Hermes, 2003](#); Scituate gneiss, S and Wamsutter Formation, W, [Fig. 2](#)) and demonstrates that these Devonian rocks extend as far west as south central Connecticut.

### **5.2. Alleghanian partial melting and magma intrusion**

The ages of zircon overgrowths identified in this study add to the growing body of data demonstrating late Paleozoic regional anatexis in southern coastal New England. Zircon grains in three of the bodies studied confirm anatexic metamorphic conditions followed by magmatic crystallization in the Early Permian. The Permian zircons from the Light House Gneiss and Narragansett Pier Granite display oscillatory and sector zoning typical of magmatic rocks. The tight cluster of zircon ages expected for magmatic rocks is obtained from the Narragansett Pier Granite ( $284 \pm 2$  Ma), but zircon ages are more scattered in the Light House Gneiss at  $\sim 292$  Ma with a higher MSWD.

Overgrowths on zircons from the Stony Creek Granite are separated from their Devonian cores by ubiquitous unconformable boundaries showing resorption of the inherited core. The round, anhedral cores demonstrate substantial zircon dissolution after the Late Devonian crystallization. The overgrowths, in turn, reflect the subsequent precipitation of zircon as the magma crystallized. The  $288 \pm 3$  Ma age of the overgrowths is consistent with a discrete magmatic crystallization event that led to the intrusion of pegmatitic, granitic, and alaskitic dikes, and migmatites ([Mikami and Digman, 1957](#); [McLellan and Stockman, 1985](#)). Several observations suggest a rather large melt fraction of the Stony Creek, Narragansett Pier, and the Light House Gneiss magmas. The low population of inherited cores, the thick Permian overgrowths, and the dominant population of large ( $>150 \mu\text{m}$ ) grains showing no inheritance at all suggest that zircon grains in the melted source rock were small, or the melt fraction was large, or both ([Watson, 1996](#)).

Many Neoproterozoic cores of the zircon grains from the Potter Hill Gneiss are preserved, with the vast majority being fractured. These cores are euhedral to subhedral and show much less resorption than zircon grains in the other three granites. Overgrowths are generally thin, on the order of a few micrometers, and the fractures in the Proterozoic cores are healed by zircon that also forms overgrowths. In spite of the ubiquitous Neoproterozoic cores, SHRIMP analyses do not resolve their age with a high precision because the analytical spots include some of the many small cracks healed by zircon with high concentrations of U, Th, and common Pb that also characterize the rims of grains. The age of the rims and fracture fillings is Early Permian ( $\sim 280$  Ma). The presence of only thin rims, and the lack of resorption of the cores suggest a minimum melt fraction ([Watson, 1996](#)) with only incipient anatexis.

### **5.3. An Alleghanian metamorphic gradient**

A trend of increasing Alleghanian metamorphic grade to the southwest exists regionally ([Zartman et al., 1970](#)) and in the Avalon terrane of Rhode Island ([Fig. 2](#)). This is well documented in the Pennsylvanian metasedimentary rocks of the Narragansett basin ([Hermes et al., 1994](#)), and as extrapolated into the crystalline rocks to the west ([Day et al., 1980](#); [Goldsmith, 1991b](#); [Attenoukon, 2009](#)). The results presented above are consistent with this overall trend. [Lundgren \(1966\)](#) mapped the second sillimanite isograd and the onset of migmatite development around the Lyme dome structurally below, and parallel to, the Honey Hill fault. Our reconnaissance and the results presented above suggest that most of the Potter Hill Gneiss lies north of the migmatite front and structurally above the more completely migmatized rocks of the Lyme dome area ([Walsh](#)

[et al., 2007](#); [Fig. 2](#)). The mineralogy of inclusions within zircon supports this anatexic event. Rims of Permian zircon from the Potter Hill Gneiss contain no inclusions detectable by the SEM. In contrast, Permian zircon grains and rims from the other three bodies analyzed contain inclusions of K-feldspar and biotite, showing that these zircons crystallized from a magma multiply saturated with these minerals near but above the solidus as predicted by anatexic melting.

### **5.4. Pulsed zircon growth**

Zircons from three of the four units analyzed show several stages of crystallization, resorption, and overgrowth. A major resorption event dissolved most protolith zircon preceding the Permian crystallization. This inference of a high melt fraction is consistent with the largely unfoliated structure of the Narragansett Pier and Light House granites that suggests emplacement of a magma with a high liquid/crystal ratio. A high zircon solubility in alkali-rich fluids is confirmed by experimental studies ([Louvel et al., 2013](#)). Resorption and overgrowth structures are also common in the Permian rims. The oscillation between dissolution and precipitation of zircon from the magma reflects varying zircon solubilities. Increasing solubility, in turn, is caused by increasing temperature, increasing alkalinity ([Louvel et al., 2013](#)), and probably decreasing pressure in any silicate liquid. Such fluctuating conditions are consistent with an active continent–continent collision, as discussed below.

### **5.5. Peri-Gondwanan inheritance**

At least a few zircon grains from all four bodies show Neoproterozoic cores. The Potter Hill Gneiss is the extreme example in which the ages of all cores are Neoproterozoic, showing that this is a Neoproterozoic unit with limited Alleghanian recrystallization. The Narragansett Pier Granite contained only a few grains with Neoproterozoic cores. However, this age is consistent with the upper intercept ages from multi-grain TIMS analyses of discordant zircons from the adjacent Avalonian gneisses ([Hermes and Zartman, 1985](#); [Zartman et al., 1988](#)). They do not support the interpretation of Archean inheritance in the Westerly Granite of [Zartman et al. \(1988\)](#). The Stony Creek and Light House granites each contain zircon with minor amounts of Neoproterozoic cores, suggesting that these magmas were derived from the melting of peri-Gondwanan lower crustal rocks. Such inheritance is consistent with a Neoproterozoic Rb–Sr whole rock age of the Stony Creek Granite ([Hills and Dasch, 1972](#)), and with Neoproterozoic ages in the range of 590–650 Ma locally and regionally ([Wintsch and Aleinikoff, 1987](#); [Walsh et al., 2007](#); [Thompson et al., 2010](#)).

The case for a Ganderian protolith of the Stony Creek Granite is the strongest. Pb and especially Nd isotopic values ( $\epsilon_{\text{Nd}}$  of  $-8$ ) of the Stony Creek Granite ([Fig. 7](#); [Table 2](#)) show an evolved source similar to rocks of the Gander terrane. Together with limited Neoproterozoic inheritance in zircon cores, and an apparent Neoproterozoic Rb–Sr whole rock age ([Hills and Dasch, 1972](#)), it is likely that this Devonian intrusion was derived from the partial melting of evolved Neoproterozoic Ganderian rocks.

### **5.6. No Acadian metamorphic event?**

No Early Devonian zircon ages have been found in either zircon cores or overgrowths to support the occurrence of an Acadian deformation in these rocks. This result is substantiated by related studies in nearby rocks ([Aleinikoff et al., 2007](#); [Walsh et al., 2007](#)). Among the 171 zircon grains analyzed and reported in [Table 1](#), none showed any evidence of crystallization in the Early Devonian. It is

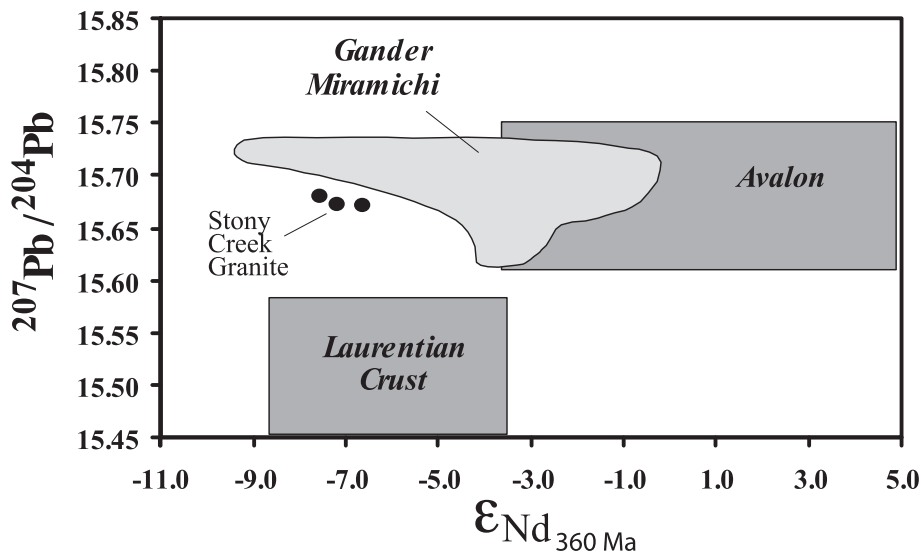


**Fig. 7.** A plot of  $^{207}\text{Pb}/^{204}\text{Pb}$  against  $\epsilon_{\text{Nd}}$  calculated at 280 Ma, showing the fields of whole rock compositions of Laurentia, Avalon, Gander-Miramichi (from Dorais et al., 2012). Three samples of Stony Creek Granite have evolved  $\epsilon_{\text{Nd}}$  values compatible with rocks of the Gander terrane, but quite incompatible with Avalon terrane rocks. These data add to the growing number of analyses of New England rocks, showing that the rocks of the Clinton dome, Massabesic Gneiss complex, and Pelham dome in Massachusetts are all compatible with a Gander terrane affinity.

unlikely that Acadian overgrowths existed and were dissolved by Alleghanian silicate liquids because older Proterozoic inherited grains have survived dissolution in each sample.

### 5.7. A cataclastic event?

In contrast to the lack of evidence for a high-grade metamorphic event in the Acadian, there is evidence that the rocks were at low metamorphic grade in the upper crust in the mid-Paleozoic. The broken and locally dismembered zircons in all these rocks reflect a Carboniferous cataclastic event. The metamorphic conditions capable of fracturing zircon are restricted to those in which the load-bearing silicates in the host rock (feldspars in this case) are also deforming by brittle fracture mechanisms, rather than by ductile processes. At normal strain rates the brittle–ductile transition in the feldspars lies in the lower amphibolite facies at about 500 °C (e.g. Rybacki and Dresen, 2004; Brander et al., 2012; Fig. 8). At higher grades feldspars would deform ductilely, leaving the stronger zircon grains undeformed, floating among these ‘softer’ feldspar grains. If quartz were load-bearing then the metamorphic conditions for cataclasis would be no higher than greenschist facies (Dunlap et al., 1997; Hirth et al., 2001).

It is significant that the fractures are present in pre-Permian cores, but rarely do they penetrate the overgrowths. Fractured inherited cores are present in all four units and are ubiquitous in the Potter Hill Gneiss that reached only incipient anatexitic conditions. The youngest fractured and healed cores, identified from the Stony Creek Granite, are ~360 Ma. This age establishes a maximum time for cataclasis. A minimum age estimate for this fracturing is established by the oldest overgrowth that also heals the fractures. This age in the Stony Creek Granite is ~288 Ma. The temperature–time window identified for the cataclasis of zircon at normal strain rates must have occurred between 360 and 290 Ma and at the temperatures <~500 °C, and possibly well into the greenschist facies.

## 6. Tectonic implications

The results above are significant for several reasons. Zircon inheritance shows that young granites south of and structurally

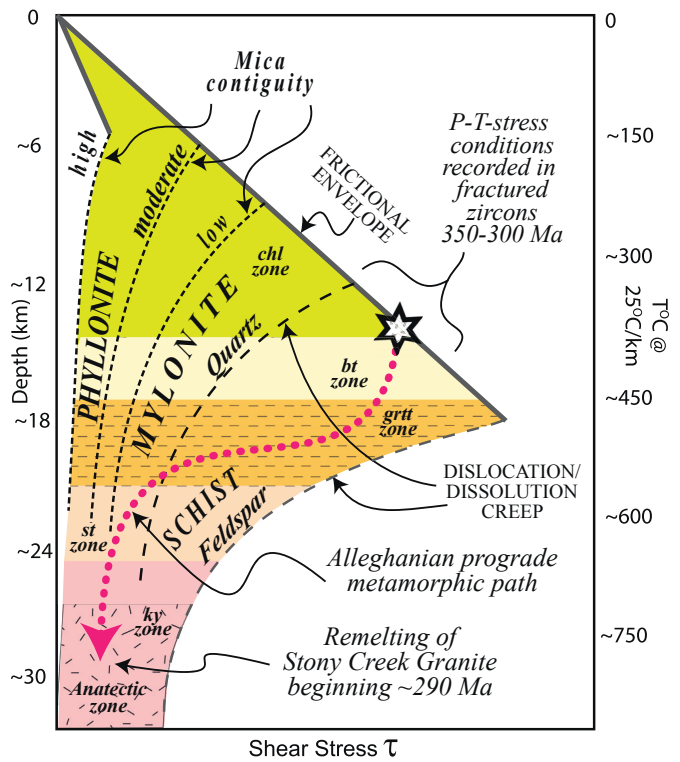


**Fig. 8.** A qualitative depth–strength diagram showing the metamorphic conditions of cataclasis of zircon (star) as argued in the text. The diagram shows the maximum shear strength supported by (fractured) crustal rocks deforming by frictional processes (FRICTIONAL ENVELOPE) and by dislocation creep (dashed curves) in several minerals (after Kohlstedt et al., 1995; Wintsch and Yeh, 2013). The prograde metamorphic path of the host granitoids from these greenschist facies to anatexitic temperatures followed the bold dotted RED line. Once anatexitic conditions were approached in the early Permian, zircon dissolved into the partial melt, and re-precipitated to heal and grow around the original zircon. The temperature scale (right) corresponds to depth at a linear 25 °C/km. Metamorphic zones are indicated: chlorite, chl; biotite, bt; garnet, grt; staurolite, st; and kyanite, ky zones. (For interpretation of the references to color in this figure legend, the reader is referred to the web version of this article.)

below the Bronson Hill terrane are derived from peri-Gondwanan rather than from Ordovician arc sources. The fractured cores of zircons show that they were relatively cool in the Carboniferous, and thus could not have been in their present position structurally below a stack of early Paleozoic anatetic nappes during Early Devonian Acadian metamorphism. The results show that even the coastal peri-Gondwanan terranes are allochthonous, implying that tectonic wedging operated in these rocks. Discussion of these points is given below.

### 6.1. Thermal histories

The identification and dating of microstructures in zircons in the peri-Gondwanan granites presented above adds a powerful constraint to the overall tectonic evolution of southeastern New England. Previous interpretations hold that Ganderian rocks accreted during the Silurian Salinic orogeny, whereas accretion of Avalonian rocks caused the Acadian orogeny (e.g. van Staal and Barr, 2012). If the rocks studied here had participated in the Acadian orogeny, then they would have been near the structural base of the Acadian section of rocks in the lower crust throughout the Late Paleozoic.

Among the several Gander cover terranes (see Fig. 2, e.g. Eusden and Barreiro, 1988; Tucker and Robinson, 1990; Wintsch et al., 1992, 1993; Robinson et al., 1998; Ague et al., 2013), the Tatnic Hill Formation near the base of the Acadian section (Sth, Fig. 2) provides the best model for the thermal history of these cover terranes. This Tatnic Hill thermal history is monitored by the bold black dashed curve of Fig. 9. Its age of deposition must be younger than its middle Silurian detrital zircons and older than the time of its anatexis revealed by the ages of metamorphic monazite and zircon (Fig. 9; Wintsch et al., 2007). After sustaining anatetic conditions throughout the Devonian, it cooled throughout the Carboniferous and Permo-Triassic as constrained by Ar/Ar ages of amphibole, muscovite, and K-feldspar (Wintsch et al., 1992; horizontal short dashed bars, Fig. 9); it was unaffected by the Alleghanian orogeny. Had the Stony Creek Granite and related granitic rocks experienced a metamorphism structurally km below the Tatnic Hill Formation, they surely would have melted. The absence of Early Devonian overgrowths provides evidence against the involvement of these peri-Gondwanan rocks in the Acadian orogeny and thus also against their occurrence at their present position at the exposed structural base of the section.

In sharp contrast, Avalonian rocks of eastern Massachusetts had been at or near the surface continuously throughout the Phanerozoic: in the Cambrian with shallow marine sediments exposed at Hoppin Hill (HH Fig. 2; Shaler et al., 1899; Goldsmith, 1991a), in the Late Devonian with volcanic rocks of the basal Wamsutta Formation (~373 Ma, Thompson and Hermes, 2003; W Fig. 2), and in the late Pennsylvanian with Stephanian A sediments (Lyons and Darrah, 1978) deposited in the Narragansett basin (NB, Fig. 2; Fig. 9). To the southwest, the Stephanian A sediments were metamorphosed to upper amphibolite facies conditions (Goldsmith, 1991b; Hermes et al., 1994; Fetherston et al., 2013). The time of peak metamorphism in southern Rhode Island is constrained to be older than the emplacement age of the Narragansett Pier Granite (~283 Ma, this study) because it contains high-grade, foliated xenoliths (Hermes et al., 1981). This occurrence, in addition to the cooling ages of amphibole and biotite immediately to the west (Dallmeyer et al., 1990; NW striped boxes, Fig. 9), constrain the cooling history of the highest-grade Pennsylvanian rocks (dot-dashed curve, Fig. 9).

The opposing temperature–time curves of Fig. 9 demonstrate that Gander cover terranes were cooling and exhuming during the Alleghanian Orogeny, at the same time that peri-Gondwanan

Gander basement rocks were heating and loading. In fact, the Stony Creek Granite must have resided in cooler upper crustal rocks where a cataclastic event fractured zircon and necessarily all framework silicates. Subsequent Permian anatexis destroyed any textural evidence of cataclasis in the feldspars, but the zircon grains have preserved it in their healed fractures. The time window for this cataclasis is the Carboniferous, but this event is plotted at the younger part of this age window in Fig. 9 so as to be consistent with the repeated healing of multiple Permian fractures (Fig. 5B). The recognition of a lower-grade, Carboniferous cataclastic event is significant because it demonstrates that the peri-Gondwanan host rocks analyzed here existed in the upper crust prior to the Alleghanian orogeny (short dashed black curve, Fig. 9), similar to those of eastern Avalon.

### 6.2. Strength of the wedge

The observation that the zircons in these granitic rocks preserve a prograde temperature–time path greatly strengthens the case for tectonic wedging of peri-Gondwanan slices into Gander cover sediments (Walsh et al., 2007; Dorais et al., 2012). The results presented here refute the argument that these high-grade rocks would be too weak to act as crustal-scale mechanical wedges. The strength of all of these granitic rocks is defined mainly by load-bearing feldspars. At realistic strain-rates their strength is mainly controlled by temperature (Rybacki and Dresen, 2004); at metamorphic grades less than lower amphibolite facies (~500 °C), these rocks would have been strong. Thus, our results establish the mechanical contrast necessary to allow tectonic wedging of Avalonia into Ganderian crust in the Alleghanian. The Stony Creek Granite, and the felsic Ganderian basement rocks it intruded, would have been cool enough and strong enough in the Carboniferous to act as a mechanical tectonic indenter. In contrast, the stack of cover rocks heated during the Acadian orogeny (above and below the Tatnic Hill Formation) would still have been warm (Fig. 9) and thus relatively weak. Moreover, many of these units are schistose with moderate biotite contents, which further weakens them (Shea and Kronenberg, 1993). Thus they would have been easily split by the cold and strong Avalon and outboard Gander wedge.

### 6.3. Geologic setting of the Avalon wedge

Recent Pb and Nd isotopic work has shown that igneous rocks of the Selden Neck indenter (SNIn, Fig. 2), were derived from primitive sources. This supports the long-standing correlation of these rocks with Avalonia (Dorais et al., 2012). In contrast, the Neoproterozoic igneous rocks exposed below the ductile Hunts Brook fault (HBF, Fig. 2) in the Lyme dome were derived from evolved crustal sources and are interpreted as being part of Ganderia (Walsh et al., 2007). Thus, the Avalonian rocks of the Selden Neck block wedged between Silurian Gander cover metasedimentary rocks and Neoproterozoic Gander basement (Wintsch et al., 2005; Walsh et al., 2007).

### 6.4. Crustal wedging

The tectonic evolution of these rocks in the Late Paleozoic is summarized in Fig. 10. The eastern part of Ganderia and apparently all of (now exposed) Avalonia were significantly outboard of Laurentia at the end of the Devonian when both terranes were intruded by Devonian granitoids. In the Early Carboniferous, Avalon began to underthrust Gander cover rocks, beginning with the composite Putnam terrane as monitored by 340 Ma amphibole cooling ages (Wintsch et al., 1992; Fig. 10). This was followed by the overthrusting of the Merrimack, Central Maine, and Bronson Hill

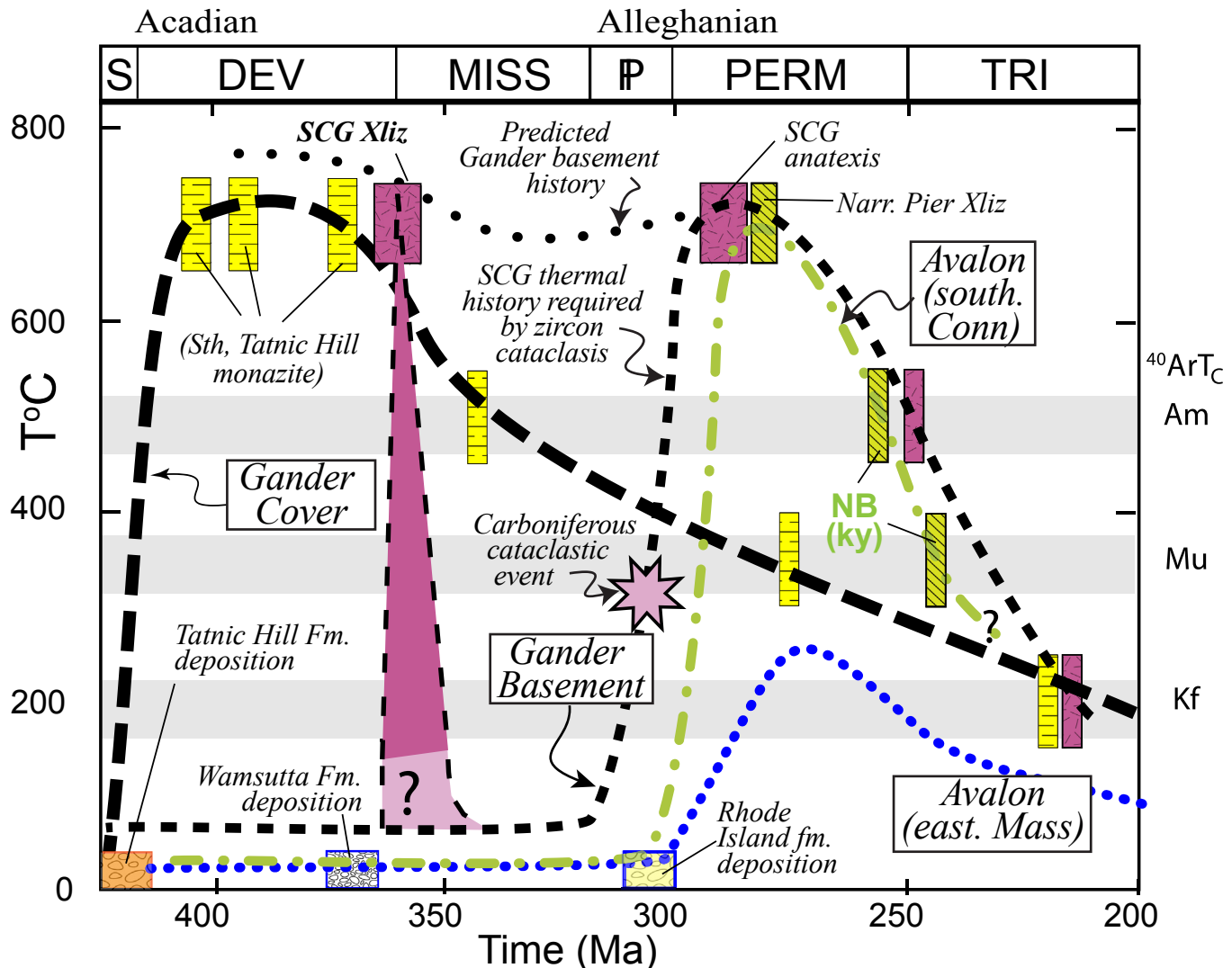


**Fig. 9.** A comparison of the thermal histories of the Avalon terrane, and Gander basement and its cover terranes compiled from several sources (see text) and modified with new information on the cataclastic zircons as interpreted here. The thermal history of the Avalon terrane of eastern Massachusetts and of southern Rhode Island is shown by the short dotted blue and dotted-dashed green lines, respectively. The thermal history of Gander basement is shown by the short dashed black line where heating is constrained by the cataclastic zircons (star). These curves show that these terranes were not heated significantly until Permian times. In contrast, Gander cover rocks (represented by rocks of the Tatnic Hill Formation, long dashed black line) were heated rapidly in the Devonian and stayed hot throughout the Devonian Acadian orogeny (Wintsch et al., 2007). The hypothesis that Gander and Avalon terrane rocks caused or at least participated in the Acadian orogeny would require them to have sustained high metamorphic grades throughout the late Paleozoic ("Predicted Gander basement history" widely spaced dotted curve, Fig. 9). On the contrary, the identification of cataclastic zircons in the Stony Creek Granite requires greenschist facies metamorphic conditions during the Carboniferous (pink star). This in turn requires an outboard position of these Gander basement rocks prior to the Alleghanian, which in turn suggests that tectonic wedging was a significant processes in the Alleghanian orogeny. Horizontal gray-green bands give the closure temperatures for argon diffusion ( $^{40}\text{ArT}_\text{C}$ ) in amphibole, muscovite, and K-feldspar (Am, Mu, Kf) respectively. (For interpretation of the references to color in this figure legend, the reader is referred to the web version of this article.)

slices as an out-of-sequence set of crystalline thrust nappes, each moving SE over each other and over the Avalon terrane (Wintsch et al., 1993) progressively through the Carboniferous and into the Permian (Fig. 10).

At the same time Ganderian rocks in the footwall of this wedge were also beginning to underthrust Bronson Hill terrane rocks even farther west. The increased thickness of this package of rocks led to partial melting and emplacement of the Hidden Lake pluton (~339 Ma, Aleinikoff et al., 2007) in the southern Bronson Hill terrane (HL, Figs. 2 and 10). The progressive approach of Gondwana throughout the late Paleozoic led to shortening and stacking of Gander cover terranes over the Avalon wedge. The toe of this wedge is now exposed as the Selden Neck indenter (SNI, Figs. 2 and 10) near the mouth of the Connecticut River.

Unexpected in this study is the occurrence of cataclastic zircons as far west as the Stony Creek and Light House granites. The limited data available (Fig. 7) suggest that at least the former was derived from evolved crustal sources consistent with Ganderia. If this is true, then not only did Avalonia wedge between Ganderian cover and basement, but some Ganderian basement itself was wedged into its own cover as far west as the western margin of the Bronson Hill terrane. The upper boundary of Neoproterozoic rocks is marked by ductile faults (Hunts Brook fault, HBft, Fig. 10B) and migmatitic rocks that would have lubricated the fault zone by melt weakening (e.g. Jamieson and Beaumont, 2013).

The western approach of these rocks was arrested by the strong Grenvillian gneisses of marginal Laurentia. After the Acadian orogeny, with a thermal peak in the early Devonian, Laurentian

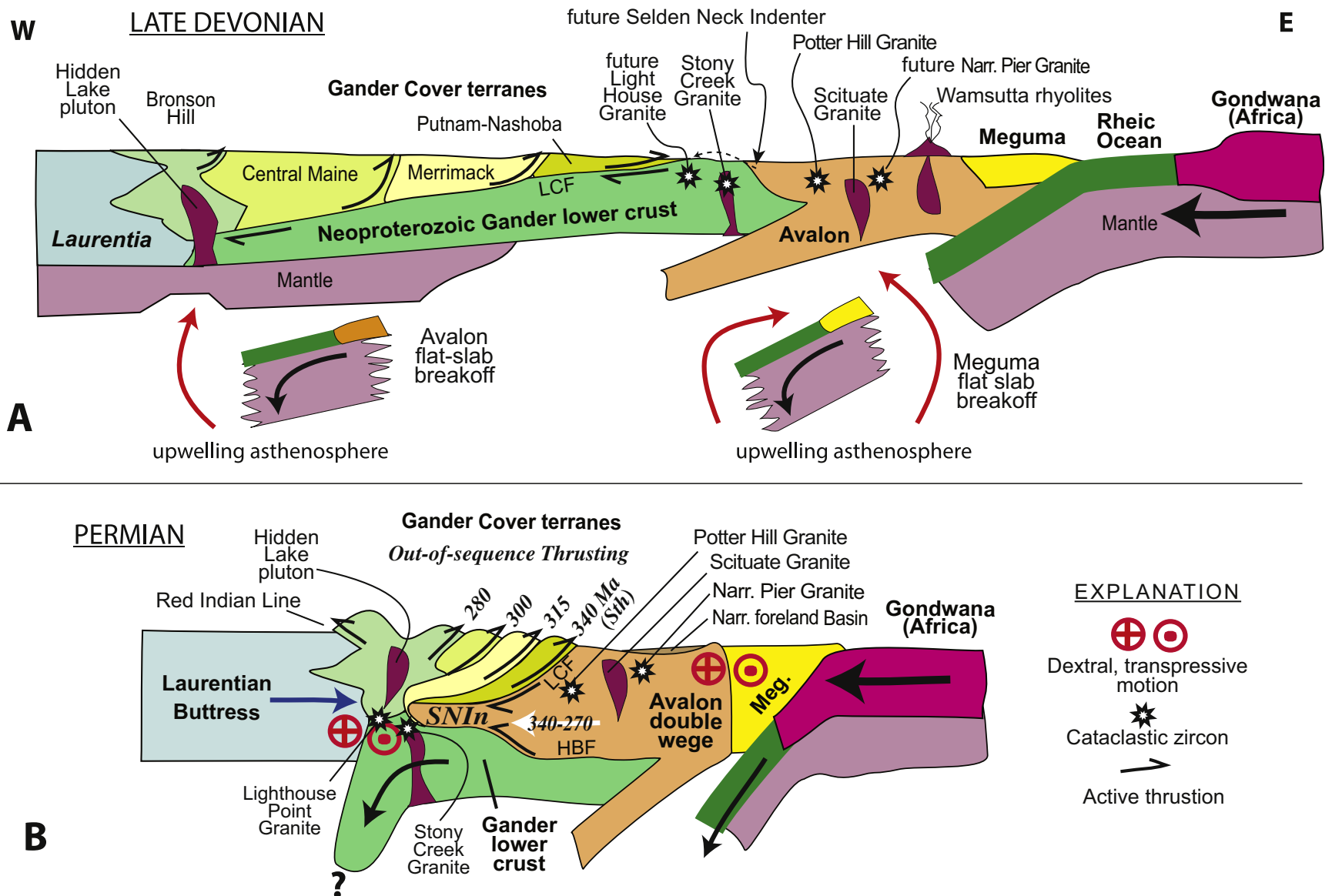


**Fig. 10.** Schematic diagrams illustrating the processes of tectonic wedging. **A.** A schematic reconstruction of the rocks of southern New England (adapted from van Staal and Barr, 2012, Fig. 16). It shows the Late Devonian Laurentian margin on the west, with the progressively accreted continental terranes to the east: Ganderia and cover terranes of Bronson Hill, Central Maine, and Putnam-Nashoba (shades of green), Avalonia (orange), Meguma (yellow) and the approaching Gondwana with its intervening Rheic Ocean. Late Devonian and Mississippian igneous rocks are shown in violet. The Ordovician Bronson Hill volcanic arc is indicated on the western margin of Ganderian Neoproterozoic lower crust, and the three Silurian metasedimentary Gander cover terranes follow to the east (see Fig. 2). **B.** A schematic cross section of southern New England constructed by unfolding the Lyme dome and restoring the gentle westerly dip of the Lake Char fault. The Selden Neck indenter (SNIn) of the Avalon terrane wedged progressively west, producing the out-of-sequence stack of thrust nappes (hornblende cooling ages given in italics; see Wintsch et al., 1993). This wedge intruded near the boundary between Gander schistose cover and its gneissic Neoproterozoic 'basement.' Stars indicate cataclastic zircons identified in this study. (For interpretation of the references to color in this figure legend, the reader is referred to the web version of this article.)

rocks cooled, such that by Carboniferous times they resided in the upper crust at greenschist facies conditions (Dietsch et al., 2010). These cool temperatures made the rocks strong enough to act as a mechanical buttress. The boundary now occupied by the Connecticut River valley acted as a transpressive margin leading to dextral strike-slip motion in southern New England in the late Paleozoic, perhaps as escape tectonics along this New York promontory (Growdon et al., 2013).

We note that our results are derived from zircons with complicated growth patterns and an intricate network of healed fractures. Many of these grains would have been rejected by geochronologists as poorly suited for isotopic analysis. However, the conclusions reached above are not dependent upon high precision data with low uncertainties. In spite of the lower precision of our data, they are sufficient to draw the orogenic-scale conclusions developed above.

## 7. Conclusions

Our study was designed to test the hypothesis that the accretion of Avalon was responsible for the Acadian orogeny in southern New England. To this end we have analyzed zircons because they are so refractory that they could survive the high temperature effects of the Permian Alleghanian orogeny and thus preserve any Early Devonian (Acadian) overgrowths. In fact, SHRIMP U–Pb geochronology reveals that no portion of any zircon in four different granitic units preserves an Early Devonian age; only Neoproterozoic cores have been identified. However, a pervasive cataclastic event is recorded in fractured and dismembered zircon cores of all four units studied here. The age of this brittle event, bracketed by the youngest fractured cores and oldest healing rims, is between ~360 and 290 Ma, or broadly, during the Carboniferous.

The occurrence of Carboniferous cataclasis indicates that: (1) these rocks were not deeply buried but were at shallow mid-crustal depths such that temperatures were low enough to allow cataclasis in feldspars and quartz of the host granites; (2) these peri-Gondwanan rocks could not have been under the Ganderian cover rocks during the high-grade Acadian metamorphism of the latter and were not present in their current structural positions during the Devonian, let alone responsible for the Acadian orogeny itself; and (3) these peri-Gondwanan rocks were accreted to Laurentia during the late Paleozoic Alleghanian orogeny. These rocks thus provide a spectacular and rare example of tectonic wedging exposed at the surface. This study shows that in addition to their geochemical and isotopic compositions, zircons can afford valuable textural and microstructural information that would normally cause them to be ignored as inappropriate for high-precision geochronology.

## Acknowledgments

The first author benefitted greatly from a warm personal and professional relationship with David Wiltschko. Dave's enthusiasm for science and for life has been a lasting inspiration. Dave's work with V. Moore helped to set the stage for our thinking in this contribution. Countless discussions with many colleagues including J. Aleinikoff, W. Bothner, D. Brown, J. Dewey, M. Kunk, P. Ryan, C. van Staal, and G. Walsh, have helped us refine our ideas. We are grateful to J. Aleinikoff, K. Ashley, C. van Staal, and an anonymous reviewer for helpful comments on an earlier draft of this manuscript, and to A. Kronenberg and R. Groshong for editorial handling. This work was partially supported by NSF grants EAR-9418203, EAR-9909410, and EAR-0510857, and by grant T33621 from the Korea Basic Science Institute.

## References

- Ague, J.J., Eckert Jr., J.O., Chu, X., Baxter, E.F., Chamberlain, C.P., 2013. Discovery of ultrahigh-temperature metamorphism in the Acadian orogen, Connecticut, USA. *Geology* 41, 271–274.
- Aleinikoff, J.N., Wintsch, R.P., Tololo, R.P., Unruh, D.M., Fanning, C.M., Schmitz, M.D., 2007. Ages and origins of rocks of the Killingworth dome, south-central Connecticut: implications for the tectonic evolution of southern New England. *Am. J. Sci.* 307, 63–118. <http://dx.doi.org/10.2475/01.2007.04>.
- Attenoukon, M.B., 2009. Ages and Origins of Metamorphic Fabrics and the Tectonics of Southeastern New England (Ph.D. thesis). Indiana University, 298 pp.
- Barrell, J., Loughlin, G.F., 1910. The Lithology of Connecticut. In: *State Geological and Natural History Survey of Connecticut Bulletin 13*, 207 pp.
- Beaumont, C., Jamieson, R.A., Nguyen, M.H., Medvedev, S., 2004. Crustal channel flows: I. Numerical models with applications to the tectonics of the Himalayan–Tibetan orogeny. *J. Geophys. Res.* 109, B06406. <http://dx.doi.org/10.1029/2003JB002809>.
- Bernold, S., 1962. Structural geometry and tectonics of gneiss doming. *Guilford, Connecticut*. *Geol. Soc. Am. Spec. Pap.* 73, 115–116.
- Bradley, D.C., 1983. Tectonics of the Acadian orogeny in New England and adjacent Canada. *J. Geol.* 91, 381–400.
- Brander, L., Svahnberg, H., Piazolo, S., 2012. Brittle-plastic deformation in initially dry rocks at fluid present conditions: transient behavior of feldspar at mid-crustal levels. *Contrib. Mineral. Petrol.* 163, 403–425.
- Dale, T.N., Gregory, H.E., 1911. The Granites of Connecticut. In: *United States Geological Survey Bulletin* 484, 137 pp.
- Dallmeyer, R.D., 1982.  $^{40}\text{Ar}/^{39}\text{Ar}$  ages from the Narragansett Basin and southern Rhode Island basement terrane; their bearing on the extent and timing of Alleghenian tectono-thermal events in New England. *Geol. Soc. Am. Bull.* 93, 1118–1130.
- Dallmeyer, R.D., Hermes, O.D., Gil-Ibarguchi, J.I., 1990.  $^{40}\text{Ar}/^{39}\text{Ar}$  mineral ages from the Scituate Granite, Rhode Island; implications for late Proterozoic tectono-thermal activity in New England. *J. Metamorph. Geol.* 82, 145–157.
- Day, H.W., Brown, V.M., Abraham, K., 1980. Precambrian(?) crystallization and Permian(?) metamorphism of hypersolvus granite in the Avalonian terrane of Rhode Island. *Geol. Soc. Am. Bull.* 91, 389–391, 1669–1741.
- Dietsch, C., Kunk, M.J., Aleinikoff, J., Sutter, J.F., 2010. The tectono-thermal evolution of the Waterbury dome, western Connecticut, based on U–Pb and  $^{40}\text{Ar}/^{39}\text{Ar}$  ages. *Geol. Soc. Am. Mem.* 206, 141–181.
- Dorais, M.J., Wintsch, R.P., Kunk, M.J., Aleinikoff, J.N., Burton, W., Underdown, C., Kerwin, C.M., 2012. P–T–t conditions, Nd and Pb isotopic compositions and detrital zircon geochronology of the Massabesic Gneiss complex, New Hampshire: isotopic and metamorphic evidence or the identification of Gander Basement, Central New England. *Am. J. Sci.* 312, 1049–1097.
- Dunlap, W.J., Hirth, G., Teyssier, C., 1997. Thermomechanical evolution of a ductile duplex. *Tectonics* 16, 983–1000.
- Eusden Jr., J.D., Barreiro, B., 1988. The timing of peak high-grade metamorphism in central-eastern New England. *Marit. Sediments Atl. Geol.* 24, 241–255.
- Feininger, T., 1964. Petrology of the Ashaway and Voluntown Quadrangles, Connecticut–Rhode Island (Ph.D. thesis). Brown University.
- Feininger, T., 1965. Bedrock Geologic Map of the Ashaway Quadrangle, Connecticut–Rhode Island. In: *United States Geological Survey Geologic Quadrangle Map GQ 403*. Scale: 1:24,000.
- Fetherston, D., Wintsch, R.P., Murray, D.P., Jones, D., 2013. Metamorphic loading and exhumation rates of the Narragansett Basin, Rhode Island. *Abstr. Progr. Geol. Soc. Am.* 45, 130.
- Foye, W.G., 1949. The Geology of Eastern Connecticut. In: *State Geological and Natural History Survey of Connecticut Bulletin 74*, p. 100.
- Goldsmith, R., 1985. Bedrock Geologic Map of the Old Mystic and Part of the Mystic Quadrangles, Connecticut, New York, and Rhode Island. In: *Miscellaneous Investigations Series, United States Geological Survey 8, 1 Sheet scale 1:24,000*.
- Goldsmith, R., 1991a. Stratigraphy of the Milford-Dedham Zone, Eastern Massachusetts; an Avalonian Terrane. In: *United States Geological Survey Professional Paper 1366*, pp. E1–E62.
- Goldsmith, R., 1991b. Structure and Metamorphic History of Eastern Massachusetts. In: *United States Geological Survey Professional Paper 1366*, pp. H1–H63.
- Gradstein, F.M., Ogg, J.G., Smith, A.G., Agterberg, F.P., Bleeker, W., Cooper, R.A., Davydov, V., Gibbard, P., Hinno, L.A., House, M.R., Lourens, L., Luterbacher, H.P., McArthur, J., Melchin, M.J., Robb, L.J., Shergold, J., Villeneuve, M., Wardlaw, B.R., Ali, J., Brinkhuis, H., Hilgen, F.J., Hooker, J., Howarth, R.J., Knoll, A.H., Laskar, J., Monechi, S., Plumb, K.A., Powell, J., Raffi, I., Röhl, U., Sadler, P., Sanfilippo, A., Schmitz, B., Shackleton, N.J., Shields, G.A., Strauss, H., Van Dam, J., van Kolfschoten, T., Veizer, J., Wilson, D., 2004. *A Geologic Time Scale 2004*: Cambridge University Press, UK, p. 589.
- Gromet, L.P., Getty, S.R., Whitehead, E.K., 1998. Late Paleozoic orogeny in southeastern New England; a mid-crustal view. In: Murray, D.P. (Ed.), *Guidebook to Fieldtrips in Rhode Island and Adjacent Regions of Connecticut and Massachusetts: New England Intercollegiate Geological Conference 90*, pp. B2.1–B2.19.
- Growdon, M.L.R., Wintsch, R.P., Kunk, M.J., 2013. Telescoping metamorphic isograds: evidence from  $^{40}\text{Ar}/^{39}\text{Ar}$  dating in the Orange–Milford complex, southern Connecticut. *Am. J. Sci.* 313, 1017–1053.
- Hermes, O.D., Zartman, R.E., 1985. Late Proterozoic and Devonian plutonic terrane within the Avalon zone of Rhode Island. *Geol. Soc. Am. Bull.* 96, 272–282.

- Hermes, O.D., Barosh, P.J., Smith, P.V., 1981. Contact relationships of the late Paleozoic Narragansett Pier Granite and country rock. In: Boothroyd, J.C., Hermes, O.D. (Eds.), Guidebook to Field Studies in Rhode Island and Adjacent Areas, New England Intercollegiate Geological Conf., 73rd Annual Meeting, University of Rhode Island, Kingston, R.I., p. 125.
- Hermes, O.D., Gromet, L.P., Murray, D.P., 1994. Bedrock Geologic Map of Rhode Island: Rhode Island Map Series No. 1. University of Rhode Island, Kingston. Scale 1:100,000.
- Hibbard, J.P., Van Staal, C.R., Rankin, D., Williams, H., 2006. Geology, Lithotectonic Map of the Appalachian Orogen, Canada–United States of America. Geological Survey of Canada. Map 2096A, scale 1:1,500,000.
- Hills, F.A., Dasch, E.J., 1972. RB/SR study of the stony creek granite, southern Connecticut; a case for limited remobilization. *Geol. Soc. Am. Bull.* 83, 3457–3463.
- Hirth, G., Teyssier, C., Dunlap, W.J., 2001. An evaluation of quartzite flow laws based on comparisons between experimentally and naturally deformed rocks. *Int. J. Earth Sci.* 90, 77–87.
- Hozik, M.J., 1988. Tectonic implications of the brittle fracture history of the Permian Narragansett Pier Granite, Rhode Island. In: Proceedings of the International Conference on Basement Tectonics 8, pp. 503–525.
- Hubbard, J., Shaw, J.H., 2009. Uplift of the Longmen Shan and Tibetan plateau, and the 2008 Wenchuan ( $M = 7.9$ ) earthquake. *Nature* 458, 194–197. <http://dx.doi.org/10.1038/nature07837>.
- Jamieson, R.A., Beaumont, C., 2013. On the origin of orogens. *Geol. Soc. Am. Bull.* 125, 1671–1702.
- Kemp, J.F., 1899. Granites of southern Rhode Island and Connecticut, with observations on Atlantic coast granites in general. *Geol. Soc. Am. Bull.* 10, 361–382.
- Kohlstedt, D.L., Evans, B., Mackwell, S.J., 1995. Strength of the lithosphere constraints imposed by laboratory experiments. *J. Geophys. Res.* 100 (B9), 17587–17602.
- Loughlin, G.F., 1912. The Gabbros and Associated Rocks at Preston, Connecticut. In: United States Geological Survey Bulletin 492, p. 158.
- Louvel, M., Sanchez Valle, C., Malfait, W.J., Testemale, D., Hazemann, J.-L., 2013. Zr complexation in high pressure fluids and silicate melts and implications for the mobilization of HFSE in subduction zones. *Geochim. Cosmochim. Acta* 104, 281–299.
- Ludwig, K.R., 2008. User's Manual for Isoplot 3.6: a Geochronological Toolkit for Microsoft Excel. Berkeley Geochronology Center Special Publication, Berkeley.
- Ludwig, K.R., 2009. User's Manual for SQUID 2. Berkeley Geochronology Center Special Publication, Berkeley.
- Lundgren Jr., Lawrence, 1966. Muscovite reactions and partial melting in southeastern Connecticut. *J. Petrol.* 7, 421–453.
- Lyons, P.C., Darrah, W.C., 1978. A late Middle Pennsylvanian flora of the Narragansett Basin, Massachusetts. *Geol. Soc. Am. Bull.* 89, 433–438.
- Martin, L.H., 1925. The Geology of the Stonington Region, Connecticut. In: State Geological and Natural History Survey of Connecticut, Bulletin 33, 70 pp.
- McLellan, E.L., Stockman, S., 1985. Age and Structural Relations of Granites, Stony Creek Area, Connecticut. In: Guidebook – State Geological and Natural History Survey of Connecticut 6, pp. 61–114.
- McLellan, E.L., Tracy, R.J., Armstrong, T.R., Miller, S.J., 1993. Migmatites of Southern New England: Melting Metamorphism and Tectonics. Geology Department, University of Massachusetts, pp. M.1–M.29. Contribution 67.
- Mikami, H.M., Digman, R.E., 1957. The Bedrock Geology of the Guilford 15-Minute Quadrangle and a Portion of the New Haven Quadrangle. In: State Geological and Natural History Survey of Connecticut Bulletin 86, p. 99.
- Moore, V., Wiltzschko, D.V., 2004. SynCollisional delamination and tectonic wedge development in convergent orogens. *Tectonics* 23, 1–27. <http://dx.doi.org/10.1029/2002TC001430> (TC2005).
- Nichols, D.R., 1956. Quadrangle Map of Bedrock of the Narragansett Pier Quadrangle. United States Geological Survey. GQ 91, scale 1:24,000.
- Paces, J.B., Miller, J.D., 1993. Precise U–Pb ages of Duluth Complex and related mafic intrusions, Northeastern Minnesota: geochronological insights to physical, petrogenetic, paleomagnetic, and tectonomagmatic processes associated with the 1.1 Ga midcontinent rift system. *J. Geophys. Res.–Solid Earth* 98, 13997–14013.
- Percival, J.G., 1842. Report on the Geology of the State of Connecticut. New Haven, Connecticut, United States, 495 pp.
- Reck, B.H., Mosher, S., 1988. Timing of intrusion of the Narragansett Pier Granite relative to deformation in the southwestern Narragansett Basin, Rhode Island. *J. Geol.* 96, 677–692.
- Robinson, P., Tucker, R.D., Bradley, D., Berry IV, H.N., Osberg, P.H., 1998. Paleozoic orogens in New England, United States of America. *GFF* 120, 119–148.
- Rodgers, J., 1985. Bedrock Geological Map of Connecticut. Connecticut Geological and Natural History Survey, Department of Environmental Protection, Hartford. Scale 1:125,000.
- Rodgers, J., Gates, R.M., Rosenfeld, J.L., 1959. Explanatory Text for the Preliminary Geological Map of Connecticut, 1956. In: State Geological and Natural History Survey of Connecticut Bulletin 84, 64 pp.
- Rybacki, E., Dresen, G., 2004. Deformation mechanism maps for feldspar rocks. *Tectonophysics* 382, 173–187.
- Sanders, J.E., 1968. Stratigraphy and structure of the metamorphic rocks of the Sachem Head anticline and related structural features, southwest of Killingworth dome, south-central Connecticut. In: Orville, P.M. (Ed.), Guidebook for Field Trips in Connecticut: Connecticut Geological and Natural History Survey Guidebook No. 2, Trip F-3, pp. 1–14.
- Shaler, N.S., Woodworth, J.B., Foerste, A.F., 1899. Geology of the Narragansett Basin. In: United States Geological Survey Monograph 33, 402 pp.
- Shea Jr., W.T., Kronenberg, A.K., 1993. Strength and anisotropy of foliated rocks with varied mica contents. *J. Struct. Geol.* 15, 1097–1121.
- Stacey, J.S., Kramers, J.D., 1975. Approximation of terrestrial Pb isotope composition by a two-stagemodel. *Earth Planet. Sci. Lett.* 26, 207–222.
- Steiger, R.H., Jäger, E., 1977. Subcommission on geochronology, convention on the use of decay constants in geo- and cosmochemistry. *Earth Planet. Sci. Lett.* vol. 36, 359–362. [http://dx.doi.org/10.1016/0012-821X\(77\)90060-7](http://dx.doi.org/10.1016/0012-821X(77)90060-7).
- Stockman, S.A., McLellan, E.L., 1987. The origin of enclaves in the Stony Creek Granite, S.E. Connecticut; stitching across a terrane boundary? *Abstr. Progr. Geol. Soc. Am.* 19, 856.
- Thompson, M.D., Hermes, O.D., 2003. Early rifting in the Narragansett Basin, Massachusetts–Rhode Island; evidence from Late Devonian bimodal volcanic rocks. *J. Geol.* 111, 597–604.
- Thompson, M.D., Ramezani, J., Barr, S.M., Hermes, O.D., 2010. High-precision U–Pb zircon dates for Ediacaran granitoid rocks in SE New England; revised magmatic chronology and correlation with other Avalonian terranes. *Geol. Soc. Am. Mem.* 206, 231–250.
- Thomson, J.A., Peterson, V.L., Berry IV, H.N., Barreiro, B., 1992. Recent Studies in the Acadian Metamorphic High, South-Central Massachusetts. In: Contribution – Geology Department, University of Massachusetts 66, pp. 229–255.
- Tucker, R.D., Robinson, P., 1990. Age and setting of the Bronson Hill magmatic arc; a re-evaluation based on U–Pb zircon ages in southern New England. *Geol. Soc. Am. Bull.* 102, 1404–1419.
- van der Velden, A.J., Van Staal, C.R., Cook, F.A., 2004. Crustal structure, fossil subduction and the tectonic evolution of the Newfoundland Appalachians: evidence from a reprocessed seismic reflection survey. *Geol. Soc. Am. Bull.* 116, 1485–1498.
- van Staal, C.R., 2005. The northern Appalachians. In: Selley, R.C., Robin, L., Cocks, M., Plimer, I.R. (Eds.), Encyclopedia of Geology. Elsevier, Oxford, pp. 81–91.
- van Staal, C.R., Barr, S., 2012. Lithospheric architecture and tectonic evolution of the Canadian Appalachians and associated Atlantic Margin. In: Clowes, R., Percival, J., Cook, F. (Eds.), Tectonic Styles in Canada: the LITHOPROBE Perspective, Geological Association of Canada Special Paper 49, pp. 42–95.
- van Staal, C.R., Whalen, J.B., Valverde-Vaquero, P., Zagorevski, A., Rogers, N., 2009. Pre-Carboniferous, episodic accretion-related, orogenesis along the Laurentian margin of the northern Appalachians. In: Murphy, J.B., Keppie, J.D., Hynes, A.J. (Eds.), Ancient Orogens and Modern Analogues, Geological Society London Special Publication 327, pp. 271–316.
- Walsh, G.J., Aleinikoff, J.N., Fanning, C.M., 2004. U–Pb geochronology and evolution of Mesoproterozoic basement rocks, western Connecticut. In: Tololo, R.P., Corriveau, L., McLellan, J., Bartholomew, M.J. (Eds.), Proterozoic Tectonic Evolution of the Grenville Orogen in North America, Geological Society of America Memoir 197, pp. 729–753. Boulder, Colorado.
- Walsh, G.J., Aleinikoff, J.N., Wintsch, R.P., 2007. Origin of the Lyme Dome and implications for the timing of multiple Alleghanian deformational and intrusive events in southern Connecticut. *Am. J. Sci.* 307, 168–215. <http://dx.doi.org/10.2475/06.2007.06>.
- Ward, F., 1909. On the lighthouse granite near New Haven, Connecticut. *Am. J. Sci.* 28, 131–142.
- Watson, E.B., 1996. Dissolution, growth and survival of zircons during crustal fusion: kinetic principles, geological models and implications for isotopic inheritance. *Spec. Pap. – Geol. Soc. Am.* 315, 43–56.
- Williams, I.S., 1998. U–Th–Pb geochronology by ion microprobe. In: McKibben, M.A., Shanks III, W.C., Ridley, W.L. (Eds.), Applications of Microanalytical Techniques to Understanding Mineralizing Processes. Society of Economic Geologists, Socorro. Rev. Econ. Geol. 7, 1–35.
- Wintsch, R.P., Sutter, J.F., 1986. A tectonic model for the late Paleozoic of southeastern New England. *J. Geol.* 94, 459–472.
- Wintsch, R.P., Aleinikoff, J.N., 1987. U–Pb isotopic evidence for late Paleozoic anatexis, deformation and possible accretion of the Avalon terrane, south-central Connecticut. *Am. J. Sci.* 277, 107–126.
- Wintsch, R.P., Sutter, J.F., Kunk, M.J., Aleinikoff, J.N., Dorais, M.J., 1992. Contrasting P–T–t paths: thermochronologic evidence for a late Paleozoic final accretion of the Avalon composite terrane in the New England Appalachians. *Tectonics* 11, 672–689. <http://dx.doi.org/10.1029/91TC02904>.
- Wintsch, R.P., Sutter, J.F., Kunk, M.J., Aleinikoff, J.N., Boyd, J.L., 1993. Alleghanian assembly of Proterozoic and Paleozoic lithotectonic terranes in south central New England: new constraints from geochronology and petrology. In: Cheney, J.T., Hepburn, T.C. (Eds.), Field Trip Guidebook for the Northeastern United States: 1993, Geological Society of America Annual Meeting, Boston, vol. 1, pp. H1–H30.
- Wintsch, R.P., Kunk, M.J., Boyd, J.L., Aleinikoff, J.N., 2003. P–T–t paths and differential Alleghanian loading and uplift of the Bronson Hill terrane, south-central New England. *Am. J. Sci.* 303, 410–446. <http://dx.doi.org/10.2475/aj.s.303.5.410>.
- Wintsch, R.P., Aleinikoff, J.N., Webster, J.R., Unruh, D.M., 2005. The Killingworth Complex: a Middle and Late Paleozoic Magmatic and Structural Dome: Guidebook for Field Trips in Connecticut. In: State Geological and Natural History Survey of Connecticut, Guidebook No. 8, pp. 305–324.
- Wintsch, R.P., Aleinikoff, J.N., Walsh, G.J., Bothner, W.A., Hussey II, A.M., Fanning, C.M., 2007. SHRIMP U–Pb evidence for a Late Silurian age of meta-sedimentary rocks in the Merrimack and Putnam-Nashoba terranes, eastern New England. *Am. J. Sci.* 307, 119–167. <http://dx.doi.org/10.2475/01.2007.05>.
- Wintsch, R.P., Aleinikoff, J.N., Walsh, G.J., 2009. Late Silurian deposition and Late Devonian metamorphism of Gander cover at the southern end of the Central Maine terrane: evidence from SHRIMP analysis of detrital zircons. *Geol. Soc. Am. Abstr. Progr.* 41 (3), 98.

- Wintsch, R.P., Yeh, Meng-Wan, 2013. Oscillating brittle and viscous behavior through the earthquake cycle in the Red River Shear Zone: reaction and textural softening and hardening. *Tectonophysics* 587, 46–62. <http://dx.doi.org/10.1016/j.tecto.2012.09.019>.
- Zartman, R.E., Hermes, O.D., 1987. Archean inheritance in zircon from late Paleozoic granites from the Avalon Zone of southeastern New England; an African connection. *Earth Planet. Sci. Lett.* 82, 305–315.
- Zartman, R.E., Hurley, P.M., Krueger, H.W., Giletti, B.J., 1970. A Permian disturbance of K–Ar radiometric ages in New England: its occurrence and cause. *Geol. Soc. Am. Bull.* 81, 3359–3374.
- Zartman, R.E., Hermes, O.D., Pease Jr., M.H., 1988. Zircon crystallization ages, and subsequent isotopic disturbance events, in gneissic rocks of eastern Connecticut and western Rhode Island. *Am. J. Sci.* 288, 376–402.